
SAFE FEEDBACK MOTION PLANNING: A CONTRACTION THEORY AND \mathcal{L}_1 -ADAPTIVE CONTROL BASED APPROACH

Arun Lakshmanan*

Mechanical Science and Engineering
University of Illinois at Urbana-Champaign
Urbana, IL 61801
lakshma2@illinois.edu

Aditya Gahlawat*

Mechanical Science and Engineering
University of Illinois at Urbana-Champaign
Urbana, IL 61801
gahlawat@illinois.edu

Naira Hovakimyan

Mechanical Science and Engineering
University of Illinois at Urbana-Champaign
Urbana, IL 61801
nhovakim@illinois.edu

ABSTRACT

Autonomous robots that are capable of operating safely in the presence of imperfect model knowledge or external disturbances are vital in safety-critical applications. In this paper, we present a planner-agnostic framework to design and certify safe tubes around desired trajectories that the robot is always guaranteed to remain inside of. By leveraging recent results in contraction analysis and \mathcal{L}_1 -adaptive control we synthesize an architecture that induces safe tubes for nonlinear systems with state and time-varying uncertainties. We demonstrate with a few illustrative examples how contraction theory-based \mathcal{L}_1 -adaptive control can be used in conjunction with traditional motion planning algorithms to obtain provably safe trajectories.

Keywords feedback motion planning, robust trajectory tracking, \mathcal{L}_1 -adaptive control, contraction theory, control contraction metrics, robust adaptive control, nonlinear reference systems.

1 Introduction

Motion planning algorithms generate optimal open-loop trajectories for robots to follow; however, any uncertainty in the system can potentially drive the robot far away from the desired path. A widely accepted approach to account for uncertainty in motion planning is through feedback [1, Chapter 8]. For instance, quadrotors experience [2] blade-flapping and induced drag forces that are dependent on its velocity, ground effect that is dependent on its height, and external wind effects that are often unaccounted for by the motion planner, since it is prohibitively expensive to perfectly model these effects, if not entirely impossible. In practice, ancillary tracking controllers or model predictive control (MPC) schemes are employed to alleviate this problem. However, the presence of the uncertainties is not explicitly considered in the control design process, and instead the performance is achieved with hand-tuned controller parameters and experimental validation. Without valid safety certificates, the uncertainty might drive the system unstable or cause it to drift far enough away from the desired trajectory, resulting in collisions with obstacles as shown in Fig. 1a.

Robust trajectory tracking controllers using classical Lyapunov stability theory have been designed for helicopters [3], hovercraft [4], marine vehicles [5], and several other autonomous robots, which exhibit nonlinear behavior. These approaches rely on backstepping techniques, sliding-mode control, passivity-based control, or other robust nonlinear control design tools [6, Chapter 14]. However, the classical methods do not provide a ‘one size fits all’ procedure for the constructive design of tracking controllers for a large class of nonlinear systems. Unless the problem has a very

*These authors contributed equally for this work

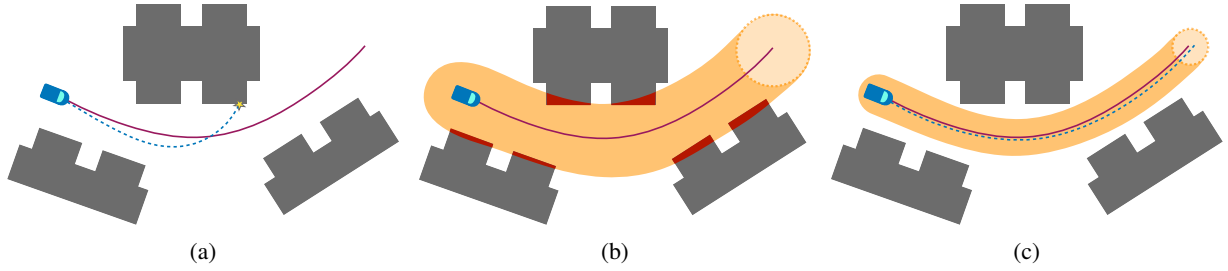


Figure 1: Although the planned path is collision free (purple), the robot’s actual trajectory (dashed-blue) might lead to a collision with the obstacles (gray) in the environment due to model discrepancies or external disturbances. (b) A feedback policy ensures that the robot stays inside of the (orange) tube which is too wide to pass between the obstacles without colliding (c) The safe feedback controller proposed in this paper guarantees that the robot’s trajectory never escapes the tube, which itself is also collision-free.

specific structure that can be exploited, a control Lyapunov function (CLF) has to be found which can be prohibitively difficult for general nonlinear systems because the feasibility conditions do not appear as linear matrix inequalities (LMI) unlike in case of linear systems.

Advances in computational resources and optimization toolboxes available to autonomous robots have led to active developments in the field of robust MPC. The two large classes of methods of interest are min-max MPC [7–9] and tube-based MPC [10–13]. Min-max MPC approaches consider the worst-case disturbance that can affect the system making them overly conservative. If the uncertainty is too large or the robot is planning over a long horizon, a min-max MPC based approach may even render the optimization infeasible. Tube-based MPC methods address these issues by employing an ancillary controller to attenuate disturbances and ensure that the robot stays inside of a ‘tube’ around the desired trajectory. However, with the exception of [13], these methods assume the existence of a stabilizing ancillary controller and its region of attraction along the desired trajectory. Moreover, the resulting tubes are of fixed width, which may be overly conservative depending on the operating conditions (see Fig. 1b). This issue is partly addressed for feedback linearizable systems in [13] by using sliding-mode boundary layer control to construct tubes of any desired size during the MPC optimization procedure. Furthermore, unlike classical methods, the MPC-based approaches while applicable to larger class of systems incur a heavy computational load and are not always amenable to real-time applications.

Contraction theory-based approaches [14, 15] bridge the gap between classical and optimization-based methods, and provide a constructive control design procedure for nonlinear systems. In [16], the authors introduce contraction analysis as tool for studying stability of nonlinear systems using differential geometry. In particular, the authors show that the ‘contracting’ or convergent nature of solutions to nonlinear systems can be derived from the differential dynamics of the system. Since the differential dynamics for nonlinear systems are of linear-time varying (LTV) form, all the results from linear systems theory can be leveraged for nonlinear systems through the contraction analysis framework. In [14], constructive control design techniques from linear systems theory can be used to find a control contraction metric (CCM), which is analogous to CLFs in the differential framework. This is significantly easier than directly finding the CLFs for nonlinear systems, because the feasibility conditions for CCMs are represented as LMIs. In [17], a design procedure for synthesizing CCM-based controllers is given, which induces fixed-width tubes in the presence of bounded external disturbances, excluding modeling uncertainties. However, as discussed before, fixed-width tubes might result in infeasibility of the problem and result in more work for the planner to find a more conservative path that produces feasible tubes. More recently, in [18] a model reference control architecture in conjunction with CCM-based feedback is proposed for handling uncertainties in the system, but without any guarantees for transient performance and robustness, which is crucial for certifying safety in robotic applications.

In this paper, we present an approach for safe feedback motion planning for control-affine nonlinear systems that relies on contraction theory-based solution for exponential stabilizability around trajectories and \mathcal{L}_1 -adaptive control for handling uncertainties and providing guarantees for transient performance and robustness. In \mathcal{L}_1 control architecture, estimation is decoupled from control, thereby allowing for arbitrarily fast adaptation subject only to hardware limitations, [19]. The \mathcal{L}_1 control has been successfully implemented on NASA’s AirStar 5.5% subscale generic transport aircraft model [20], Calspan’s Learjet [21], and unmanned aerial vehicles [22, 23]. In [24], the authors presented the analysis for the \mathcal{L}_1 -adaptive control architecture with nonlinear time-varying reference systems. However, the stabilizability of the nominal nonlinear model and associated safety certificates were simply assumed. In this paper, we present a constructive design of feedback strategy for nonlinear systems using CCMs and \mathcal{L}_1 -adaptive control that pro-

vides strong guarantees of transient performance and robustness for a large class of control-affine nonlinear systems. Furthermore, we show how this control architecture induces tubes that can be flexibly changed to ensure safety based on the uncertainty in the system and the environment. In particular, this flexibility is provided by the architecture of the \mathcal{L}_1 -adaptive control by decoupling the control loop from the estimation loop [19]. In this way, the width of the certifiable tubes can be adjusted allowing the safe operation of a robot in tight confines.

The manuscript is organized as follows. The problem statement and the assumptions are provided in Section 2. A brief introduction to contraction theory is provided in Section 3. The proposed controller is presented in Section 4 and the stability analysis of the closed-loop system is provided in Section 5. Finally, in Section 6 the results of numerical experimentation are provided.

Notation

The notation in this paper follows typical conventions used in the controls and robotics communities, but we list a few operations and terms explicitly in this section. The set of non-negative reals is denoted by $\mathbb{R}_{\geq 0}$. The set of real matrices is denoted by $\mathbb{R}^{m \times n}$ with dimensions $m, n \in \mathbb{N}$. The set of real symmetric matrices is denoted by $\mathbb{S}^n \subset \mathbb{R}^{n \times n}$. We denote an $n \times n$ identity matrix by \mathbb{I}_n and a m -column vector of ones by $\mathbb{1}_m$. Given any matrix $R \in \mathbb{R}^{n \times n}$, $[R]_{\mathbb{S}} = (R + R^T) / 2 \in \mathbb{S}^n$ denotes its symmetric part.

The largest and smallest eigenvalue for a square matrix A is denoted by $\bar{\lambda}(A)$ and $\underline{\lambda}(A)$ respectively. The positive definiteness of a square matrix A is given by the inequality $A \succ 0$. We denote the Pontryagin set difference between two sets $\mathcal{A} \subseteq \mathcal{C}$ and $\mathcal{B} \subseteq \mathcal{C}$ as $\mathcal{A} \ominus \mathcal{B}$. The $|\cdot|$ represents the absolute value of a scalar and $\|\cdot\|$ represents the Euclidean norm for vectors and induced vector norm for matrices, unless otherwise denoted. The Laplace transform and its inverse of a function $f(t)$ is denoted by $\mathcal{L}[f(t)]$ and $\mathcal{L}^{-1}[f(t)]$ respectively. Given a matrix-valued function $M(x) \in \mathbb{R}^{n \times n}$ and a vector-valued function $f(x) \in \mathbb{R}^n$, we denote the directional derivative of $M(x)$ with respect to $f(x)$ by $\partial_f M(x) = \sum_{i=1}^n (\partial M(x) / \partial x_i) f_i(x)$, where $f_i(x)$ is the i^{th} element of $f(x)$.

We denote by $\mathcal{L}_{\infty}(S)$ the set of functions $f : S \subset \mathbb{R} \rightarrow \mathbb{R}^n$ which satisfy $\|f\|_{\mathcal{L}_{\infty}} = \sup_{x \in S} \|f(x)\| < \infty$, where $\|\cdot\|$ is a Euclidean norm. Additionally, for any $g \in \mathcal{L}_{\infty}(\mathbb{R}_{\geq 0})$ we define the truncated \mathcal{L}_{∞} -norm as $\|g\|_{\mathcal{L}_{\infty}}^{[0, \tau]} = \sup_{t \in [0, \tau]} \|g(t)\| < \infty$. We denote by $\mathcal{L}_1(S)$ the set of functions $f : S \subset \mathbb{R} \rightarrow \mathbb{R}^n$ satisfying $\|f\|_{\mathcal{L}_1} = \int_S \|f(x)\| dx < \infty$. For any $g \in \mathcal{L}_1(\mathbb{R}_{\geq 0})$, the truncated \mathcal{L}_1 norm is defined analogously.

2 Problem Statement

We consider systems for which the evolution of dynamics can be represented as

$$\dot{x}(t) = F(x(t), u(t)) \quad (1a)$$

$$= f(x(t)) + B(x(t))(u(t) + h(t, x(t))), \quad (1b)$$

with initial condition $x(0) = x_0$, where $x(t) \in \mathbb{R}^n$ is the system state and $u(t) \in \mathbb{R}^m$ is the control input. The functions $f(x) \in \mathbb{R}^n$ and $B(x) \in \mathbb{R}^{n \times m}$ are known, and $h(t, x) \in \mathbb{R}^m$ represents the uncertainties. The *unperturbed/nominal dynamics* ($h \equiv 0$) are therefore represented as

$$\dot{x}(t) = \bar{F}(x(t), u(t)) \quad (2a)$$

$$= f(x(t)) + B(x(t))u(t), \quad x(0) = x_0. \quad (2b)$$

Consider a *desired control trajectory* $u^*(t) \in \mathbb{R}^m$ and the induced *desired state trajectory* $x^*(t) \in \mathbb{R}^n$ from any planner based on unperturbed/nominal dynamics

$$\dot{x}^*(t) = \bar{F}(x^*(t), u^*(t)), \quad x^*(0) = x_0. \quad (3)$$

Together, $(x^*(t), u^*(t))$ is referred to as the *desired state-input trajectory pair*. The planner ensures that the desired state-trajectory $x^*(t)$ remains in a compact *safe set* $\mathcal{X} \subset \mathbb{R}^n$, for all $t \geq 0$.

The goal is to design a control input $u(t)$ so that the state $x(t)$ of the uncertain system in (1) remains ‘close’ to the desired trajectory $x^*(t)$ while also ensuring $x(t) \in \mathcal{X}$, for all $t \geq 0$. In order to rigorously define the notion of ‘closeness’, we need the following definition:

Definition 2.1. Given a positive scalar ρ and the desired state trajectory $x^*(t)$, $\Omega(\rho, x^*(t))$ denotes the ρ -norm ball around $x^*(t)$, i.e.

$$\Omega(\rho, x^*(t)) = \{y \in \mathbb{R}^n \mid \|y - x^*(t)\| \leq \rho\}. \quad (4)$$

Clearly, $\Omega(\rho, x^*(t))$ induces a *tube* centered around $x^*(t)$ given by $\bigcup_{t \geq 0} \Omega(\rho, x^*(t))$ with ρ as the radius.

The problem under consideration can now be stated as follows: Given the desired trajectory $x^*(t) \in \mathcal{X}$ and a positive scalar ρ , design a control input $u(t)$ such that the state of the uncertain system (1) satisfies:

$$x(t) \in \Omega(\rho, x^*(t)) \subset \mathcal{X}, \quad \forall t \geq 0.$$

Note the condition that $\Omega(\rho, x^*(t)) \subset \mathcal{X}$ is dependent on the desired trajectory $x^*(t)$ (given by the planner) and the tube width ρ (chosen by the user). To ensure that this control-independent condition is satisfied, we place the following assumption.

Assumption 2.1. *Given the positive scalar ρ , the desired state trajectory satisfies $x^*(t) \in \mathcal{X}_\rho$, for all $t \geq 0$, where*

$$\mathcal{X}_\rho = \mathcal{X} \ominus \mathcal{P}(\rho), \quad \mathcal{P}(\rho) = \{y \in \mathbb{R}^n \mid \|y\| \leq \rho\}, \quad (5)$$

in which \ominus denotes the Pontryagin set difference.

Remark 2.1. *The implication of Assumption 2.1 is that if the state trajectory satisfies $x(t) - x^*(t) \in \mathcal{P}(\rho)$ and $x^*(t) \in \mathcal{X}_\rho$, for all $t \geq 0$, then the definition of the Pontryagin set difference implies that $x(t) \in \Omega(\rho, x^*(t)) \subset \mathcal{X}$, for all $t \geq 0$.*

Assumption 2.2. *The desired control/input trajectory satisfies*

$$\|u^*(t)\| \leq \Delta_{u^*}, \quad \forall t \geq 0,$$

with the upper bound Δ_{u^*} known.

Note that the bound Δ_{u^*} is a function of the planner, which provides the desired state-input trajectory in (3). Next, we place assumptions on the boundedness and continuity properties of the system functions and uncertainties.

Assumption 2.3. *The known functions $f(x) \in \mathbb{R}^n$ and $B(x) \in \mathbb{R}^{n \times m}$ are locally bounded and continuously differentiable, satisfying*

$$\begin{aligned} \|f(x)\| &\leq \Delta_f, \quad \left\| \frac{\partial f(x)}{\partial x} \right\| \leq \Delta_{f_x}, \quad \|B(x)\| \leq \Delta_B, \\ \sum_{i=1}^n \left\| \frac{\partial B(x)}{\partial x_i} \right\| &\leq \Delta_{B_x}, \quad \forall x \in \mathcal{X}, \end{aligned}$$

with the bounds being known.

Assumption 2.4. *The uncertainty $h(t, x)$ is bounded and continuously differentiable in both x and t , thus satisfying*

$$\|h(t, x)\| \leq \Delta_h, \quad \left\| \frac{\partial h(t, x)}{\partial x} \right\| \leq \Delta_{h_x}, \quad \left\| \frac{\partial h(t, x)}{\partial t} \right\| \leq \Delta_{h_t},$$

for all $x \in \mathcal{X}$ and $t \geq 0$, where the bounds are assumed to be known.

Assumption 2.5. *The input gain matrix $B(x)$ has full column rank. Furthermore, the Moore-Penrose inverse of $B(x)$ defined as $B^\dagger(x) = (B^\top(x)B(x))^{-1} B^\top(x)$ satisfies the following bounds*

$$\|B^\dagger(x)\| \leq \Delta_{B^\dagger}, \quad \sum_{i=1}^n \left\| \frac{\partial B^\dagger(x)}{\partial x_i} \right\| \leq \Delta_{B_x^\dagger}, \quad \forall x \in \mathcal{X}.$$

3 Preliminaries on Contraction Theory

Contraction theory allows to synthesize feedback laws so that, in the absence of uncertainties, the state of the unperturbed/nominal dynamics in (2) tracks a feasible desired trajectory $x^*(t)$. We begin with the notion of incremental exponential stabilizability.

Definition 3.1 ([17]). Consider a desired state-input trajectory pair $(x^*(t), u^*(t))$ satisfying Eq. (3). Suppose there exist scalars $\lambda, R > 0$ and a feedback operator $k_c : \mathbb{R}^n \times \mathbb{R}^n \rightarrow \mathbb{R}^m$ such that the trajectory $x(t)$ of the unperturbed dynamics $\dot{x}(t) = \bar{F}(x(t), u_c(t))$ with control $u(t) = u^*(t) + k_c(x^*(t), x(t))$ satisfies

$$\|x^*(t) - x(t)\| \leq R e^{-\lambda t} \|x^*(0) - x(0)\|, \quad \forall t \geq 0.$$

Then, the trajectory $x^*(t)$ is said to be *Incrementally Exponentially Stabilizable (IES)* with rate λ and overshoot R .

Alternatively, one may instead use the notion of *universal exponential stabilizability* if Definition 3.1 holds for any pair $(x^*(t), u^*(t))$ satisfying the nominal/unperturbed dynamics in (2) [14].

With the notion of IES defined, we now proceed to examine how IES may be established for a given system. For the compact safe set $\mathcal{X} \subset \mathcal{R}^n$ defined in Section 2, let $T_x\mathcal{X}$ be the tangent space of \mathcal{X} at $x \in \mathcal{X}$. Consequently, we denote by $T\mathcal{X} = \dot{\bigcup}_{x \in \mathcal{X}} T_x\mathcal{X}$ the tangent bundle of \mathcal{X} , where $\dot{\bigcup}$ denotes the disjoint union. Details on differential geometric notions used in the manuscript may be found in [25]. The variational dynamics of the unperturbed/nominal system in (2) may be written as [26, Chapter 3]

$$\dot{\delta}_x = \left(\frac{\partial f(x)}{\partial x} + \sum_{j=1}^m u[j] \frac{\partial b_j(x)}{\partial x} \right) \delta_x + B(x) \delta_u, \quad (6)$$

with $\delta_x(0) = x_0$ and where we have dropped the temporal dependencies for brevity. Here, $\delta_x(t) \in T_{x(t)}\mathcal{X}$, $\delta_u(t) = T_{u(t)}\mathbb{R}^m$, $u[j](t)$ is the j^{th} element of the control vector and $b_j(x) \in \mathbb{R}^n$ is the j^{th} column of $B(x)$.

Definition 3.2. Consider the differential dynamics in (6). Suppose there exist positive scalars $\lambda, \underline{\alpha}, \bar{\alpha}$, $0 < \underline{\alpha} < \bar{\alpha} < \infty$, and a smooth² function $M : \mathbb{R}^n \rightarrow \mathbb{S}^n$ such that, for all $(x, \delta_x) \in T\mathcal{X}$,

$$\underline{\alpha} \mathbb{I}_n \preceq M(x) \preceq \bar{\alpha} \mathbb{I}_n, \quad (7a)$$

$$\delta_x^\top M(x) B(x) = 0 \Rightarrow$$

$$\delta_x^\top \left(\partial_f M(x) + \left[M(x) \frac{\partial f(x)}{\partial x} \right]_{\mathbb{S}} + 2\lambda M(x) \right) \delta_x \leq 0, \quad (7b)$$

$$\partial_{b_j} M(x) + \left[M(x) \frac{\partial b_j(x)}{\partial x} \right]_{\mathbb{S}} = 0, \quad j \in \{1, \dots, m\}. \quad (7c)$$

Then, the function $M(x)$ is defined to be the *Control Contraction Metric (CCM)* for the nominal/unperturbed dynamics (2).

Theorem 3.1 ([14, 17]). *Given positive scalars λ , and $\underline{\alpha} \leq \bar{\alpha} < \infty$, suppose there exists a CCM $M(x)$ for the nominal/unperturbed dynamics in Eq. (2). Then, given any desired state-input trajectory $(x^*(t), u^*(t))$ as in Eq. (3), there exists a feedback operator $k_c : \mathbb{R}^n \times \mathbb{R}^n \rightarrow \mathbb{R}^m$ such that the trajectory $x(t)$ of the unperturbed dynamics $\dot{x}(t) = \bar{F}(x(t), u_c(t))$ with control $u(t) = u^*(t) + k_c(x^*(t), x(t))$ is IES with respect to $x^*(t)$ in the sense of Definition 3.1.*

The central idea to this result is that the function $V(x, \delta_x)$ can be interpreted as a differential Lyapunov function and the conditions in Eq. (7) ensure that $\dot{V}(x, \delta_x) \leq -2\lambda V(x, \delta_x)$ for all $(x, \delta_x) \in T\mathcal{X}$. We place the following assumption on the known/unperturbed dynamics.

Assumption 3.1. *The nominal/unperturbed dynamics in Eq. (2) admit a CCM $M(x)$ with positive scalars $\lambda, \underline{\alpha}$, and $\bar{\alpha}$, as in Definition 3.2.*

Using Theorem 3.1 it is straightforward to conclude that the consequence of this assumption is that any feasible state-input trajectory can be tracked by the nominal/unperturbed dynamics in the sense of Definition 3.1 with rate λ and overshoot $R = \bar{\alpha}/\underline{\alpha}$. Given any $p, q \in \mathcal{X}$, let $\gamma : [0, 1] \rightarrow \mathcal{X}$ be the minimizing geodesic between the points. Then, using $M(x)$ as a Riemannian metric on \mathcal{X} , the Riemannian energy of γ is given by

$$\mathcal{E}(p, q) = \int_0^1 \gamma_s(s)^\top M(\gamma(s)) \gamma_s(s) ds, \quad (8)$$

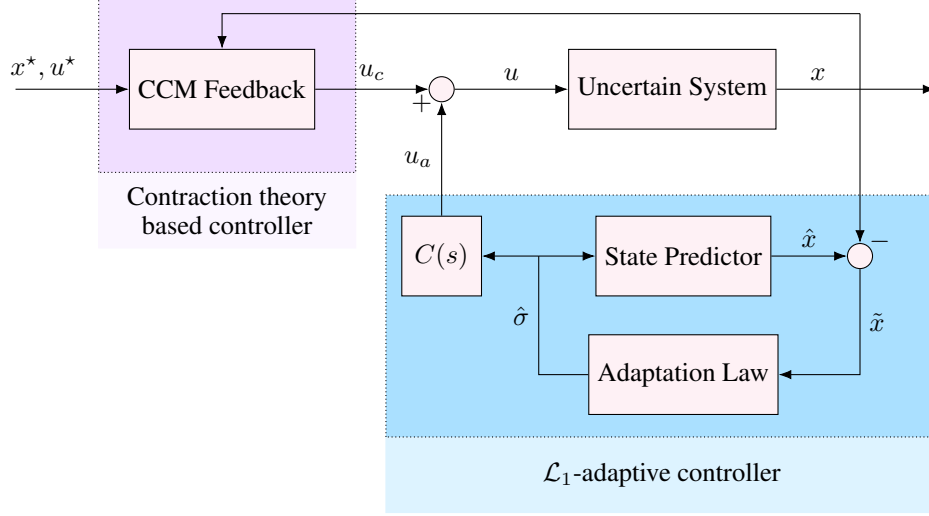
where $\gamma_s(s) = \partial \gamma(s) / \partial s$. Existence of the minimizing geodesic is guaranteed by the Hopf-Rinow theorem. Further details on Riemannian geometry may be found in [27]. A direct and straightforward consequence of Assumption 3.1 is that

$$\underline{\alpha} \|p - q\|^2 \leq \mathcal{E}(p, q) \leq \bar{\alpha} \|p - q\|^2, \quad \forall p, q \in \mathcal{X}. \quad (9)$$

We will rely on the Riemannian energy's interpretation as a control Lyapunov function for the presented methodology. This interpretation was initially presented in [14].

Remark 3.1. *Thus far we have only established the existence of feedback control operators and not constructed any. In fact, as explained in [14, Sec. VI.A], any controller may be chosen as long as a set membership is established. The precise choice of the controller we use will be presented later in the manuscript.*

²Throughout the manuscript, by smooth we mean the class \mathcal{C}^∞ of functions defined on appropriate domains.


 Figure 2: Architecture of CCM-based \mathcal{L}_1 -adaptive control

4 Contraction Theory Based \mathcal{L}_1 -Adaptive Control

In this section we introduce the structure of the proposed controller for the uncertain nonlinear system in Eq. (1). Consider the following feedback decomposition

$$u(t) = u_c(t) + u_a(t), \quad (10)$$

where $u_c : \mathbb{R}_{\geq 0} \rightarrow \mathbb{R}^m$ is the contraction theory based control designed to guarantee IES (Definition 3.1) of the nominal dynamics in Eq. (2), and $u_a : \mathbb{R}_{\geq 0} \rightarrow \mathbb{R}^m$ is the \mathcal{L}_1 control signal. The overall architecture of the proposed feedback is illustrated in Fig. 2. We refer to the uncertain system in Eq. (1) with the feedback law Eq. (10) as the \mathcal{L}_1 closed-loop system. We now define the individual components of the control law.

4.1 Contraction theory based control: $u_c(t)$

As mentioned in Section 3, under Assumption 3.1, Theorem 3.1 guarantees the existence of a feedback law which renders the nominal dynamics in Eq. (2) IES. In particular, we propose the following law

$$u_c(t) = u^*(t) + k_c(x^*(t), x(t)), \quad (11)$$

where, for the feedback term, we use the law constructed in [17, Sec. 5.1], which is the solution to the following QP:

$$k_c(x^*(t), x(t)) = \arg \min_{k \in \mathbb{R}^m} \|k\|^2, \quad (12a)$$

$$\begin{aligned} \text{s.t. } & 2\gamma_s^\top(1, t)M(x(t))\dot{x}_k(t) - 2\gamma_s^\top(0, t)M(x^*(t))\dot{x}^*(t) \\ & \leq -2\lambda\mathcal{E}(x^*(t), x(t)), \end{aligned} \quad (12b)$$

in which $M(\cdot)$ is the CCM (Definition 3.2), $\gamma(s, t)$, $s \in [0, 1]$, is the minimizing geodesic with $\gamma(1, t) = x_k(t)$ and $\gamma(0, t) = x^*(t)$. As previously defined, the desired state-input pair satisfies $\dot{x}^*(t) = \bar{F}(x^*(t), u^*(t))$ with the nominal dynamics defined in Eq. (2). Additionally, $\dot{x}_k(t) = \bar{F}(x_k(t), u^*(t) + k)$.

Remark 4.1. As explained by the authors in [17, Sec. 5.1], the solution to the QP in (12) can be obtained analytically given the minimizing geodesic $\gamma(\cdot, t)$. Alternatively, one may use the differential controller proposed in [14], albeit at the expense of an increase in the control effort.

4.2 \mathcal{L}_1 -adaptive control: $u_a(t)$

The computation of the signal $u_a(t)$ depends on three components illustrated in Fig. 2, namely, the state-predictor, the adaptation law, and a low-pass filter. Similar to [9], we define the *state-predictor* as

$$\dot{\hat{x}}(t) = \bar{F}(x(t), u_c(t) + u_a(t) + \hat{\sigma}(t)) + A_m \tilde{x}(t), \quad (13)$$

with $\tilde{x}(0) = x_0$, and where $\tilde{x}(t) \in \mathbb{R}^n$ is the state of the predictor, $\tilde{x}(t) = \hat{x}(t) - x(t)$ is the state prediction error, and $A_m \in \mathbb{R}^{n \times n}$ is an arbitrary Hurwitz matrix.

The uncertainty estimate $\hat{\sigma}(t)$ in Eq. (13) is governed by the following adaptation law

$$\dot{\hat{\sigma}}(t) = \text{Proj}_{\mathcal{H}}(\hat{\sigma}(t), -B(x)^\top P \tilde{x}(t)), \quad \hat{\sigma}(0) \in \mathcal{H}, \quad (14)$$

where $\Gamma > 0$ is the adaptation rate, $\mathcal{H} = \{y \in \mathbb{R}^m \mid \|y\| \leq \Delta_h\}$ is the set to which the uncertainty estimate is restricted to remain in with Δ_h defined in Assumption 2.4. Furthermore, $\mathbb{S}^n \ni P \succ 0$, is the solution to the Lyapunov equation $A_m^\top P + P A_m = -Q$, for some $\mathbb{S}^n \ni Q \succ 0$. Moreover, $\text{Proj}_{\mathcal{H}}(\cdot, \cdot)$ is the projection operator standard in adaptive control literature [28], [29].

Finally, the control law $u_a(t)$ is defined as the following Laplace transform

$$u_a(s) = -C(s)\hat{\sigma}(s), \quad (15)$$

where $C(s)$ is a low-pass filter with bandwidth ω . Note that there is an abuse of notation when we denote both the geodesic interval parameter and the Laplace variable by s . The delineation between the two is clear from the context.

4.3 Filter bandwidth and adaptation rate

The design of the \mathcal{L}_1 -adaptive controller involves the design of a strictly proper and stable low-pass filter $C(s)$ with $C(0) = \mathbb{I}_m$. Let the bandwidth of this filter be ω . In the manuscript, for the sake of simplicity, we choose $C(s) = \frac{s}{s+\omega} \mathbb{I}_m$. As we will see in Section 5, the bandwidth ω of the low-pass filter $C(s)$ in Eq. (15) and the adaptation rate Γ in Eq. (14) are design parameters which can be thought of as ‘tuning-knobs’. However, these entities need to satisfy a few conditions mentioned below. The reasoning behind these conditions will be made clear in the subsequent section.

Suppose that Assumption 3.1 holds. Then, for arbitrarily chosen positive scalars ϵ and ρ_a , define

$$\rho = \rho_r + \rho_a = \sqrt{\frac{\bar{\alpha}}{\underline{\alpha}}} \|x_0^* - x_0\| + \epsilon + \rho_a. \quad (16)$$

Furthermore, suppose that Assumptions 2.1-2.5 hold. Define

$$\begin{aligned} \zeta_1(\omega) &= \frac{2\Delta_z}{\underline{\alpha}} \\ &= 2\rho\Delta_B \frac{\bar{\alpha}}{\underline{\alpha}} \left(\frac{\Delta_h}{|2\lambda - \omega|} + \frac{\Delta_{h_t} + \Delta_{h_x}\Delta_{\dot{x}_r}}{2\lambda\omega} \right), \end{aligned} \quad (17a)$$

$$\zeta_2(\omega) = \bar{\alpha}\Delta_{\Psi_x} \left(\frac{\Delta_h}{|2\lambda - \omega|} + \frac{\Delta_{h_t} + \Delta_{h_x}\Delta_{\dot{x}_r}}{2\lambda\omega} \right), \quad (17b)$$

$$\zeta_3(\omega) = \bar{\alpha}\Delta_{h_x} \left(\frac{4\lambda\Delta_B + \Delta_{\dot{\Psi}}}{\lambda\omega} \right), \quad (17c)$$

where $\Delta_{\dot{x}_r}$, Δ_{Ψ_x} , and $\Delta_{\dot{\Psi}}$, are known positive scalars which will be defined later in the analysis. Then, the bandwidth ω of the low-pass filter $C(s)$ and the adaptation rate need to verify the following conditions

$$\rho_r^2 \geq \frac{\mathcal{E}(x_0^*, x_0)}{\underline{\alpha}} + \zeta_1(\omega), \quad (18a)$$

$$\underline{\alpha} > \zeta_2(\omega) + \zeta_3(\omega), \quad (18b)$$

$$\sqrt{\Gamma} > \frac{\Delta_\theta}{\rho_a(\underline{\alpha} - \zeta_2(\omega) - \zeta_3(\omega))}, \quad (18c)$$

where Δ_θ is another known positive scalar defined later in the analysis.

Remark 4.2. Based on the definition of ρ_r in Eq. (16) and the bounds on the Riemannian energy $\mathcal{E}(x^*(t), x(t))$ in Eq. (9), the inequality $\rho_r^2 > \mathcal{E}(x_0^*, x_0)/\underline{\alpha}$ holds. Furthermore, since $\zeta_1(\omega)$, $\zeta_2(\omega)$, and $\zeta_3(\omega)$, all converge to zero as ω increases, the bandwidth conditions in (18a)-(18b) can always be satisfied by choosing a large enough ω .

5 Performance Analysis

In this section we analyze the performance of the uncertain system in Eq. (1) with the \mathcal{L}_1 control feedback $u(t)$ defined in Eq. (10). As in [9], to derive the bounds between the desired trajectory $x^*(t)$ and the state $x(t)$ of the uncertain

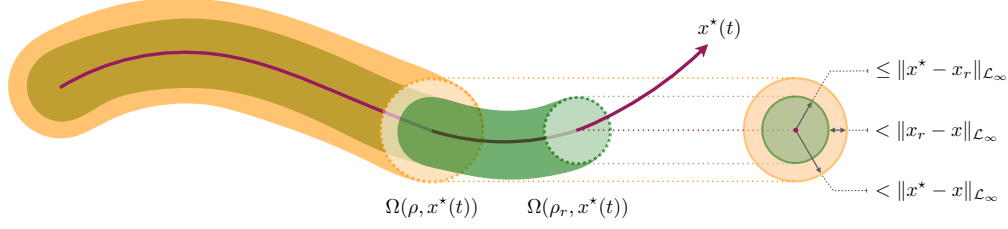


Figure 3: The bounds/tubes for the analysis of the CCM based \mathcal{L}_1 -adaptive controller.

system, we first introduce the following intermediate system, which we refer to as the *reference system*:

$$\begin{aligned}\dot{x}_r(t) &= F(x_r(t), -\eta_r(t)) \\ &= f(x_r(t)) + B(x_r(t))(-\eta_r(t) + h(t, x_r(t))),\end{aligned}\quad (19a)$$

$$\eta_r(s) = C(s)\mathcal{L}[h(t, x_r(t))], \quad x_r(0) = x_0. \quad (19b)$$

The main feature of the reference system is the cancellation of the uncertainty $h(t, x_r(t))$ only within the bandwidth of the low-pass filter.

The analysis consists of two parts: we first derive bounds between the desired trajectory and the reference system $\|x^*(t) - x_r(t)\|$. Then we derive the bounds between the states of the reference system and the actual system $\|x_r(t) - x(t)\|$. Recall that we refer to the actual system as the \mathcal{L}_1 closed loop system, which is given by Eq. (1) with the control law in Eq. (10). Finally, the triangle inequality then produces the desired bound on $\|x^*(t) - x(t)\|$. In this way, the reference system behaves as an ‘anchor system’ for the analysis. These bounds are illustrated in Fig. 3. Furthermore, we provide the justification of treating the bandwidth ω of $C(s)$ and the adaptation rate Γ as tuning-knobs. Indeed, the upcoming analysis will show that we can ensure that $x(t) \in \Omega(\rho, x^*(t))$ (see Eq. (4)) for all $t \geq 0$.

We begin with the bound between the reference system state and desired state trajectory. This corresponds to the green tube in Fig. 3. The proofs for all the claims in this section are provided in Appendix A.

Lemma 5.1. *Let all the assumptions hold and let ρ_r be as defined in Eq. (16). If the conditions in (18a)-(18b) hold, then for any desired state trajectory $x^*(t)$, the state $x_r(t)$ of the reference system in (19) satisfies*

$$x_r(t) \in \Omega(\rho_r, x^*(t)), \quad \forall t \geq 0, \quad (20)$$

and is uniformly ultimately bounded as

$$x_r(t) \in \Omega(\mu(\omega, T), x^*(t)) \subsetneq \Omega(\rho_r, x^*(t)), \quad \forall t \geq T > 0, \quad (21)$$

where the ultimate bound is defined as

$$\mu(\omega, T) := \sqrt{\frac{e^{-2\lambda T} \mathcal{E}(x_0^*, x_0)}{\underline{\alpha}}} + \zeta_1(\omega). \quad (22)$$

Next, we compute the bounds between the reference system in Eq. (19) and the \mathcal{L}_1 closed-loop system (Eq. (1) with Eq. (10)).

Lemma 5.2. *Suppose that the stated assumptions and the conditions in Eq. (18) hold. Additionally, assume that the trajectory of the \mathcal{L}_1 closed-loop system $x(t) \in \Omega(\rho, x^*(t))$, for all $t \in [0, \tau]$, with $\Omega(\rho, x^*(t))$ and ρ defined in Eq. (4) and Eq. (16), respectively. Then,*

$$\|x_r - x\|_{\mathcal{L}_\infty}^{[0, \tau]} < \rho_a,$$

where ρ_a is given in Eq. (16).

We now use Lemmas 5.1-5.2 to state the main result of the paper.

Theorem 5.1. *Suppose that the stated assumptions and conditions in Eq. (18) hold. Consider a desired state trajectory $x^*(t)$ as in (3) and the state of the \mathcal{L}_1 closed-loop system defined via (1) and (10). Then,*

$$x(t) \in \Omega(\rho, x^*(t)), \quad \forall t \geq 0, \quad (23)$$

and is uniformly ultimately bounded as

$$x(t) \in \Omega(\delta(\omega, T), x^*(t)) \subsetneq \Omega(\rho, x^*(t)), \quad \forall t \geq T > 0. \quad (24)$$

Here, the ultimate bound is defined as

$$\delta(\omega, T) := \mu(\omega, T) + \rho_a, \quad (25)$$

where the positive scalars ρ and ρ_a are defined in (16), and $\mu(\omega, T)$ is defined in Lemma 5.1.

Discussion

A few critical comments are in order for the performance analysis. The main result in Theorem 5.1 provides uniform ultimate bounds. Let us first discuss the implication of the uniform bound ρ in Eq. (23). As per the definition in Eq. (16), $\rho = \rho_r + \rho_a$. It is evident from the definition that ρ is lower bounded by the initial condition difference $\|x_0^* - x_0\|$ and the positive scalars $\underline{\alpha}$ and $\bar{\alpha}$ which are associated with the CCM $M(x)$ of the nominal dynamics. Furthermore, as per the proof of Lemma 5.2, since $\rho_a \propto 1/\sqrt{\Gamma}$, the adaptation rate Γ can be increased to the maximum value allowable by the computation hardware to guarantee the smallest ρ_a , and thus, the smallest uniform bound ρ . However, the fact remains that the uniform bound ρ guaranteed by the \mathcal{L}_1 -controller for the tracking remains lower bounded by $\|x_0^* - x_0\|$. The only way this bound can be further reduced is if the underlying planner which provides the desired state-input pair $(x^*(t), u^*(t))$ can minimize $\|x_0^* - x_0\|$.

Theorem 5.1 also provides the (uniform) ultimate bound via $\delta(\omega, T)$ defined in Eq. (25). As already mentioned, $\rho_a \propto 1/\sqrt{\Gamma}$. Furthermore, from the definition of $\zeta_1(\omega)$ in Eq. (17a), it is evident that by choosing a large enough ω , there will always exist a known $0 < T < \infty$ such that $\delta(\omega, t) \leq \bar{\rho}$, for all $t \geq T$, for any chosen $\bar{\delta} > 0$. Therefore, we can always arbitrarily shrink the tube $\bigcup_{t \geq 0} \Omega(\bar{\delta}, x^*(t))$ by choosing appropriate bandwidth ω and rate of adaptation Γ . This feature of the CCM-based \mathcal{L}_1 -controller is very advantageous, since, for example, this capability will allow the safe navigation of a robot through tight and cluttered environments. This improved performance, however, comes at the cost of reduced robustness. There exists a trade-off between performance and robustness that should be taken into consideration. As aforementioned, performance (radius of tubes around $x^*(t)$) depends on Γ and ω . The rate of adaptation Γ is obviously limited by the available computational hardware. More importantly, the role of the low-pass filter $C(s)$ in the \mathcal{L}_1 -control architecture (Fig. 2) is to decouple the control loop from the estimation loop [19]. Thus, increasing the bandwidth ω of $C(s)$ in order to get a tighter tube will lead to the $u_a(t)$ component of the \mathcal{L}_1 -input to behave as a high-gain signal, thus possibly sacrificing desired robustness levels [30]. Therefore, this trade-off must always be taken into account during the planning phase.

6 Simulation Results

We provide two illustrative examples. In the first example, we consider the non-feedback linearizable system from [14] and synthesize the controller to ensure safe regulation around the equilibrium point. We also show the effect of uniform ultimate bounds discussed in the previous section, if the system were to start far away from the equilibrium. In the second example, we consider the system from [31] and ensure safety in a motion planning context during trajectory tracking. In particular we show how altering the tube parameters affects the choice in the filter bandwidth and adaptation rate.

6.1 Non-feedback Linearizable Systems

Consider the system with the structure defined in Eq. (1) and the system functions given by

$$f(x) = \begin{bmatrix} -x_1(t) + x_3(t) \\ x_1^2(t) - 2x_1(t)x_2(t) - x_2(t) + x_3(t) \\ -x_2(t) \end{bmatrix}, B = \begin{bmatrix} 0 \\ 0 \\ 1 \end{bmatrix},$$

where the state $x(t) = [x_1(t) \ x_2(t) \ x_3(t)]^\top$. A dual metric of the form $W(x(t)) = W_0 + W_1x_1(t) + W_2x_1^2(t)$ can be found using sum-of-squares programming. More details about the (dual) metric and the procedure for its synthesis can be found in [14] and [32]. Now, suppose that the system is experiencing sinusoidal disturbances of the form: $h(t) = 0.1 \sin(2t)$. We chose the initial condition of the system as $x_0 = [1 \ -1 \ 1]^\top \times 10^{-2}$ and the target state as $x^* = [0 \ 0 \ 0]^\top$. A pure CCM-based feedback strategy produces the oscillatory behavior, seen in Fig. 4a. A CCM-based \mathcal{L}_1 -adaptive controller is designed in Fig. 4b for tube widths $\epsilon = 0.05$ and $\rho_a = 0.02$. The filter bandwidth and adaptation rate required to achieve this level of performance were found to be $\omega = 40$ and $\Gamma = 2 \times 10^7$ respectively. Notice that the bounds are far more conservative than the actual behavior of the system. In fact, the error in tracking is uniformly bounded by $\|x\|_{\mathcal{L}_\infty} < 0.02$.

6.2 Safe Tubes for Motion Planning

Consider the system with the structure defined in Eq. (1) and the system functions given by

$$f(x) = \begin{bmatrix} -x_1(t) + 2x_2(t) \\ -0.25x_2^3(t) - 3x_1(t) + 4x_2(t) \end{bmatrix}, \quad B = \begin{bmatrix} 0.5 \\ -2 \end{bmatrix},$$

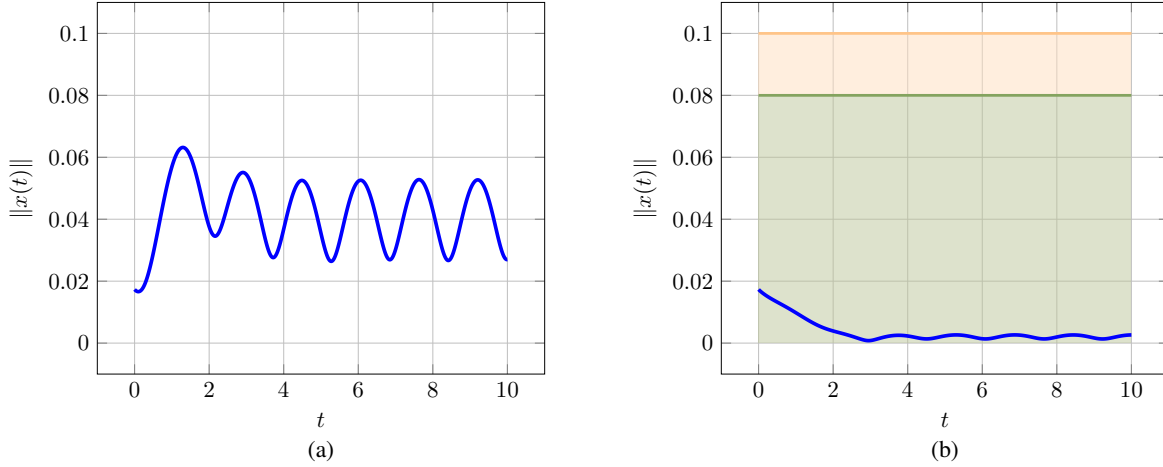


Figure 4: Comparison of controller performance between (a) pure CCM-based feedback, and a (b) CCM-based \mathcal{L}_1 architecture. The green and orange shaded regions signify the induced $\Omega(\rho_r, x^*)$ and $\Omega(\rho, x^*)$ tubes respectively.

where the state $x(t) = [x_1(t) \ x_2(t)]^\top$. Since this particular system is feedback linearizable, it admits a constant (or flat) dual metric for all $x \in \mathbb{R}^2$ [15]. The value of the dual metric can be found in [31]. Suppose the system is affected by uncertainties of the form: $h(t, x) = -2 \sin(2t) - 0.1 \|x(t)\|$, consisting of both time and state dependent terms. Depending on the desired level of tracking performance or closeness to obstacles in the environment, the user will pick the tube parameters ϵ and ρ_a as defined in Eq. (16). In Fig. 5, we illustrate the trade-offs between choosing a tighter ϵ (Fig. 5a) versus a tighter ρ_a (Fig. 5c) for this system.

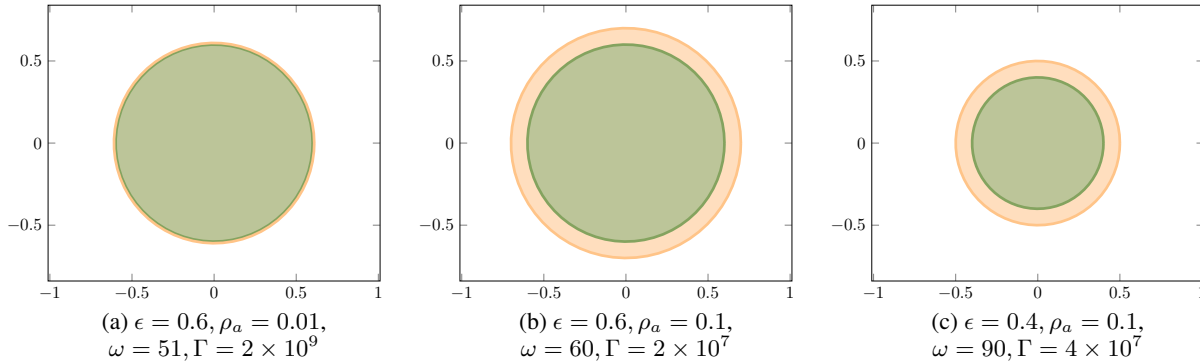


Figure 5: Relationship between the choice of tube parameters ϵ and ρ_a and the controller parameters ω and Γ through the conditions defined in Eq. (18). For clarity the initial conditions for the desired trajectory and the actual system in this illustration are assumed to be the same.

In Fig. 6b, we observe the performance and robustness benefits of using CCM-based \mathcal{L}_1 -adaptive control. Not only does the system track the desired trajectory closely, but also avoids colliding with obstacles (unlike in Fig. 6a) through an appropriate choice of tube parameters.

7 Conclusion and Future Work

We present a control methodology to enable safe and guaranteed feedback motion planning. The presented work relies on differential geometric contraction theory and \mathcal{L}_1 -adaptive control. The proposed controller enables the apriori computation of uniform and ultimate-bounds which act as safety-certificates. These safety certificates induce ‘tubes’ which can be taken into account by any planner of choice. In this way, the safety of the system/robot is always guaranteed in the presence of model and environmental uncertainties. Furthermore, by using the control law’s filter bandwidth and rate of adaptation as tuning knobs, the width of the safety tubes can be adjusted. Future research will deal with

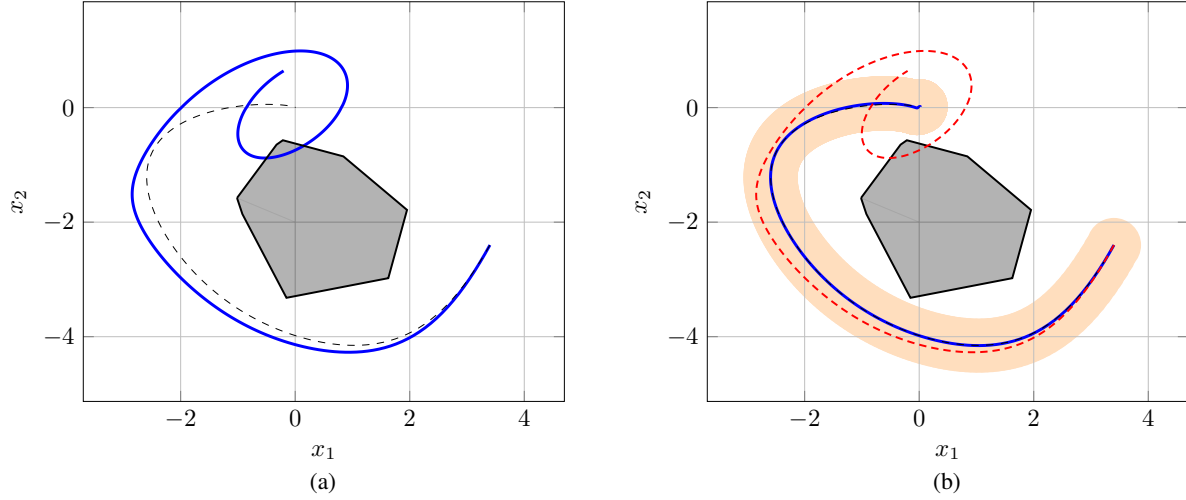


Figure 6: Comparison of performance and robustness between (a) pure CCM-based feedback, and (a) CCM-based \mathcal{L}_1 architecture with tube parameters $\epsilon = 0.4$ and $\rho_a = 0.1$. The dashed black line shows the desired trajectory designed by a planner, the gray polygon is an obstacle, and the orange shaded region is the safe tube given by $\Omega(\rho, x^*(t))$. The behavior of the system under pure CCM-based feedback has been overlaid as a dashed red line in (b) for clarity.

the incorporation of learning into the proposed control framework. This will lead to improved performance since the underlying planner will have access to improved model knowledge. More importantly, the controller proposed in this work will keep the learning process safe because of the bounds during the transient phase. Further investigations will be undertaken to extend this framework to enable safe planning and control using a reduced-order model to enable fast planning.

Acknowledgements

This work is financially supported by Air Force Office of Scientific Research (AFOSR), National Aeronautics and Space Administration (NASA) and National Science Foundation's National Robotics Institute (NRI) and Cyber Physical Systems (CPS) awards #1830639 and #1932529. We would also like to thank Dr. Riccardo Bonalli for fruitful discussions regarding the proof for Lemma B.4, and Dr. Evangelos Theodorou for introducing us to world of stochastic contraction theory [33] which will be especially useful in future work.

Appendix

A Main Results

In this appendix we provide the proofs of the claims in the manuscript.

Proof of Lemma 5.1. We have $\|x^*(0) - x_r(0)\| = \|x_0^* - x_0\| < \rho_r$ since $\epsilon > 0$ and $\frac{\bar{\alpha}}{\alpha} \geq 1$. We show that $\|x^* - x_r\|_{\mathcal{L}_\infty} \leq \rho_r$ by contradiction. Assume that the lemma statement does not hold; then since x_r and x^* are continuous, there must exist a $\tau^* > 0$ such that

$$\begin{aligned} \|x^*(\tau^*) - x_r(\tau^*)\| &= \rho_r, \\ \|x^*(t) - x_r(t)\| &< \rho_r, \quad t \in [0, \tau^*). \end{aligned}$$

Consider the minimizing geodesic $\bar{\gamma}(s, t)$ such that $\bar{\gamma}(0, t) = x^*(t)$ and $\bar{\gamma}(1, t) = x_r(t)$. Then the time derivative of the Riemannian energy is given by

$$\begin{aligned} \frac{1}{2} \dot{\mathcal{E}}(x^*, x_r) &= \bar{\gamma}_s(s, t)^\top M(\bar{\gamma}(s, t)) \dot{\bar{\gamma}}(s, t) \Big|_{s=0}^{s=1} \\ &= \bar{\gamma}_s(1, t)^\top M(x_r) \dot{x}_r(t) - \bar{\gamma}_s(0, t)^\top M(x^*) \dot{x}^*(t). \end{aligned}$$

Substituting the reference and desired system dynamics into the equation above we obtain

$$\begin{aligned} \frac{1}{2}\dot{\mathcal{E}}(x^*, x_r) &= \bar{\gamma}_s(1, t)^\top M(x_r) (f(x_r) + B(x_r)u_c(t, x_r)) + \bar{\gamma}_s(1, t)^\top M(x_r) (B(x_r)(h(t, x_r) - \eta_r(t))) \\ &\quad - \bar{\gamma}_s(0, t)^\top M(x^*) (f(x^*) + B(x^*)u^*(t)). \end{aligned} \quad (\text{A.1})$$

As shown in [18, Lemma 1], since the uncertainty is matched with the control channel, the metric M designed for the unperturbed system satisfies the stronger CCM conditions for the real system. This implies that the CCM-based feedback controller is exponentially convergent with rate λ and, moreover, from [17, Theorem 3.2], the time derivative of the Riemannian energy satisfies

$$\bar{\gamma}_s(1, t)^\top M(x_r) (f(x_r) + B(x_r)u_c(t, x_r)) - \bar{\gamma}_s(0, t)^\top M(x^*) (f(x^*) + B(x^*)u^*(t)) \leq -\lambda \mathcal{E}(x^*, x_r).$$

Substituting into Eq. (A.1) produces

$$\frac{1}{2}\dot{\mathcal{E}}(x^*, x_r) \leq -\lambda \mathcal{E}(x^*, x_r) + \bar{\gamma}_s(1, t)^\top M(x_r) B(x_r) (h(t, x_r) - \eta_r(t)).$$

Integrating both sides of the equation above, we have

$$\mathcal{E}(x^*, x_r) \leq e^{-2\lambda t} \mathcal{E}(x_0^*, x_0) + 2 \int_0^t e^{-2\lambda(t-\nu)} \bar{\gamma}_s(1, t)^\top M(x_r) B(x_r) (h(\nu, x_r) - \eta_r(\nu)) d\nu.$$

The integral term can be expressed as the solution to the following virtual scalar system

$$\dot{z}(t) = -2\lambda z(t) + \bar{\gamma}_s(1, t)^\top M(x_r) B(x_r) \xi(t), \quad z(0) = 0, \quad (\text{A.2})$$

$$\xi(s) = (1 - C(s)) \mathcal{L}[h(t, x_r)]. \quad (\text{A.3})$$

Note that from Lemmas B.3 and B.5 and Assumptions 2.3 and 2.4 the following bounds hold for all $x_r(t) \in \Omega(\rho_r, x^*(t)) \subset \Omega(\rho, x^*)$ (since $\rho_r < \rho$) and all $t \in [0, \tau^*]$:

$$\begin{aligned} \|\bar{\gamma}_s(1, t) M(x_r) B(x_r)\| &\leq \rho \bar{\alpha} \Delta_B, \quad \|h(t, x_r)\| \leq \Delta_h, \\ \left\| \dot{h}(t, x_r) \right\| &= \left\| \frac{\partial h(t, x_r)}{\partial t} + \frac{\partial h(t, x_r)}{\partial x} \dot{x}_r(t) \right\| \leq \Delta_{h_t} + \Delta_{h_x} \Delta_{\dot{x}_r}. \end{aligned}$$

Then the solution of a linear system of the form in Eqs. (A.2) and (A.3) satisfies the following norm bound from Lemma B.1

$$\|z(t)\| \leq \rho \bar{\alpha} \Delta_B \left(\frac{\Delta_h}{|2\lambda - \omega|} + \frac{\Delta_{h_t} + \Delta_{h_x} \Delta_{\dot{x}_r}}{2\lambda \omega} \right) \triangleq \Delta_z.$$

From the definition of the Riemannian energy in Eq. (8) and [17, Lemma 3.7] it follows that

$$\underline{\alpha} \|x^*(t) - x_r(t)\|^2 \leq \mathcal{E}(x^*, x_r) \leq e^{-2\lambda t} \mathcal{E}(x_0^*, x_0) + 2\Delta_z.$$

In our contradiction argument, we had that $\|x^*(\tau^*) - x(\tau^*)\| = \rho_r$. Therefore the following inequality must be satisfied

$$\rho_r^2 \leq \frac{1}{\underline{\alpha}} (e^{-2\lambda \tau^*} \mathcal{E}(x_0^*, x_0) + 2\Delta_z) < \frac{\mathcal{E}(x_0^*, x_0)}{\underline{\alpha}} + \frac{2\Delta_z}{\underline{\alpha}}, \quad (\text{A.4})$$

for some $\tau^* > 0$. However, from Eq. (18a) the bandwidth is chosen such that

$$\rho_r^2 \geq \frac{\mathcal{E}(x_0^*, x_0)}{\underline{\alpha}} + \zeta_1(\omega) = \frac{\mathcal{E}(x_0^*, x_0)}{\underline{\alpha}} + \frac{2\Delta_z}{\underline{\alpha}}.$$

This directly contradicts our earlier statement. Therefore, $\|x_r - x^*\|_{\mathcal{L}_\infty} \leq \rho_r$. Moreover, from Eq. (A.4) we also obtain the following uniform ultimate bound

$$\|x^*(t) - x_r(t)\| \leq \sqrt{\frac{e^{-2\lambda T} \mathcal{E}(x_0^*, x_0)}{\underline{\alpha}} + \zeta_1(\omega)},$$

for all $t \geq T \geq 0$. □

Proof of Lemma 5.2. We prove this lemma by contradiction. Assume that

$$\|x_r - x\|_{\mathcal{L}_\infty}^{[0, \tau]} \geq \rho_\gamma.$$

Since $x_r(0) = x(0)$, there exists a $\tau^* \in (0, \tau]$ such that

$$\begin{aligned} \|x_r(\tau^*) - x(\tau^*)\| &= \rho_\gamma, \\ \|x_r(t) - x(t)\| &< \rho_\gamma, \quad t \in [0, \tau^*). \end{aligned}$$

Let $\gamma(s, t)$ be the minimizing geodesic between x_r and x such that $\gamma(1, t) = x_r(t)$ and $\gamma(0, t) = x(t)$. Consider the Riemannian energy $\mathcal{E}(x_r, x)$ between x_r and x . Then the time derivative of the Riemannian energy is given by [27]

$$\begin{aligned} \frac{1}{2} \dot{\mathcal{E}}(x_r, x) &= \bar{\gamma}_s(s, t)^\top M(\bar{\gamma}(s, t)) \dot{\bar{\gamma}}(s, t) \Big|_{s=0}^{s=1} \\ &= \gamma_s(1)^\top M(x_r) \dot{x}_r - \gamma_s(0)^\top M(x) \dot{x}. \end{aligned}$$

Substituting in the dynamics, we get

$$\begin{aligned} \frac{1}{2} \dot{\mathcal{E}}(x_r, x) &= \gamma_s(1)^\top M(x_r) [f(x_r) + B(x_r)(u_c(t, x_r) + h(t, x_r) - \eta_r(t))] \\ &\quad - \gamma_s(0)^\top M(x) [f(x) + B(x)(u_c(t, x) + h(t, x) - \hat{\eta}(t))]. \end{aligned}$$

Similar to the reasoning used in Lemma 5.1, the metric M designed for the ideal system also satisfies the stronger CCM conditions for the real system [18, Lemma 1]. This implies that the nominal parts of the system are contracting, given by

$$\frac{1}{2} \dot{\mathcal{E}}(x_r, x) \leq -\lambda \mathcal{E}(x_r, x) + \Psi(x_r)^\top (h(t, x_r) - \eta_r(t)) - \Psi(x)^\top (h(t, x) - \hat{\eta}(t)),$$

where $\Psi(x_r) := B(x_r)^\top M(x_r) \bar{\gamma}_s(1, t)$ and $\Psi(x) := B(x)^\top M(x) \bar{\gamma}_s(0, t)$ are introduced for clarity. By adding and subtracting terms on the right-hand side we obtain

$$\begin{aligned} \frac{1}{2} \dot{\mathcal{E}}(x_r, x) &\leq -\lambda \mathcal{E}(x_r, x) + (\Psi(x_r) - \Psi(x))^\top (h(t, x_r) - \eta_r(t)) + \Psi(x)^\top (h(t, x_r) - \eta_r(t) - h(t, x) + \eta(t)) \\ &\quad + \Psi(x)^\top (\hat{\eta}(t) - \eta(t)). \end{aligned}$$

Since $h(t, x_r) - \eta_r(t) = \mathcal{L}^{-1}[(1 - C(s))\mathcal{L}[h(t, x_r)]]$, $h(t, x) - \eta(t) = \mathcal{L}^{-1}[(1 - C(s))\mathcal{L}[h(t, x)]]$, and $\hat{\eta}(t) - \eta(t) = \tilde{\eta}(t)$, we can rewrite the equation above as

$$\frac{1}{2} \dot{\mathcal{E}}(x_r, x) \leq -\lambda \mathcal{E}(x_r, x) + \Phi_1(x_r, x) + \Phi_2(x_r, x) + \Phi_3(x_r, x), \quad (\text{A.5})$$

where

$$\begin{aligned} \Phi_1(x_r, x) &:= (\Psi(x_r) - \Psi(x))^\top \mathcal{L}^{-1}[(1 - C(s))\mathcal{L}[h(t, x_r)]], \\ \Phi_2(x_r, x) &:= \Psi(x)^\top \mathcal{L}^{-1}[(1 - C(s))\mathcal{L}[h(t, x_r) - h(t, x)]], \\ \Phi_3(x_r, x) &:= \Psi(x)^\top \tilde{\eta}(t). \end{aligned}$$

Solving the differential equation in Eq. (A.5) above we obtain

$$\mathcal{E}(x_r, x) \leq 2 \int_0^t e^{-2\lambda(t-\nu)} (\Phi_1(x_r, x) + \Phi_2(x_r, x) + \Phi_3(x_r, x)) d\nu \quad (\text{A.6})$$

Notice that $\|\Psi(x_r) - \Psi(x)\|$ satisfies the following bounds

$$\|\Psi(x_r) - \Psi(x)\| \leq \|B(x_r)^\top - B(x)^\top\| \|M(x_r) \bar{\gamma}_s(1, t)\| + \|B(x)^\top\| \|M(x_r) \bar{\gamma}_s(1, t) - M(x) \bar{\gamma}_s(0, t)\|.$$

Since $x_r(t) \in \Omega(\rho_r, x^*(t))$ from Lemma 5.1 and $x(t) \in \Omega(\rho, x^*(t))$ for all $t \in [0, \tau]$ by assumption, the bounds from Lemmas B.3 and B.4 and Assumption 2.3 hold and we obtain the following inequality

$$\|\Psi(x_r) - \Psi(x)\| \leq \frac{1}{2} \bar{\alpha} \Delta_{\Psi_x} \|x_r(t) - x(t)\|^2,$$

which holds for all $t \in [0, \tau]$ and where

$$\Delta_{\Psi_x} := 2\Delta_{B_x} + \frac{\Delta_B \Delta_{M_x}}{\bar{\alpha}}. \quad (\text{A.7})$$

Here, we define Δ_{M_x} as a scalar which satisfies

$$\sum_{i=1}^n \left\| \frac{\partial M}{\partial x_i}(x) \right\| \leq \Delta_{M_x}, \quad \forall x \in \Omega(\rho, x^*(t)), \quad (\text{A.8})$$

which is guaranteed to exist due to the assumed smoothness of the CCM $M(x)$ for all $t \in [0, \tau]$. Additionally, from Assumptions 2.3 and 2.4 and Lemmas B.3 and B.7 we know that the following inequalities hold

$$\begin{aligned} \|h(t, x_r)\| &\leq \Delta_h, \quad \|\dot{h}(t, x_r)\| \leq \Delta_{h_t} + \Delta_{h_x} \Delta_{\dot{x}_r}, \quad \|h(t, x_r) - h(t, x)\| \leq \Delta_{h_x} \|x_r(t) - x(t)\|, \\ \|\Psi(x)\| &\leq \bar{\alpha} \Delta_B \|x_r(t) - x(t)\|, \quad \|\dot{\Psi}(x)\| \leq \Delta_{\dot{\Psi}}, \end{aligned}$$

for all $t \in \tau$. In order to derive bounds on Eq. (A.6), define the following scalar trajectories

$$z_1(t) := \int_0^t e^{-2\lambda(t-\nu)} \Phi_1(x, x_r) d\nu, \quad z_2(t) := \int_0^t e^{-2\lambda(t-\nu)} \Phi_2(x, x_r) d\nu.$$

Then, the functions $z_i, i \in \{1, 2\}$, are the states of the following systems

$$\dot{z}_i(t) = -2\lambda z_i(t) + b_i(t) \xi_i(t), \quad z_i(0) = 0, \quad (\text{A.9a})$$

$$\xi_i(s) = (1 - C(s)) \sigma_i(s), \quad (\text{A.9b})$$

where

$$\begin{aligned} b_1(t) &= \Psi(x_r) - \Psi(x), \quad \sigma_1(t) = h(t, x_r), \\ b_2(t) &= \Psi(x), \quad \sigma_2(t) = h(t, x_r) - h(t, x). \end{aligned}$$

From our initial assumption $\|x_r(t) - x(t)\| \leq \rho_\gamma$ for $t \in [0, \tau^*]$. Using Lemma B.1 for the $z_1(t)$ system and Lemma B.2 for the $z_2(t)$ system we have the following bounds

$$\|z_1(t)\| \leq \frac{1}{2} \zeta_2(\omega) \rho_\gamma^2, \quad \|z_2(t)\| \leq \frac{1}{2} \zeta_3(\omega) \rho_\gamma^2,$$

for all $t \in [0, \tau^*]$, and where

$$\begin{aligned} \zeta_2(\omega) &= \bar{\alpha} \Delta_{\Psi_x} \left(\frac{\Delta_h}{|2\lambda - \omega|} + \frac{\Delta_{h_t} + \Delta_{h_x} \Delta_{\dot{x}_r}}{2\lambda\omega} \right) \\ \zeta_3(\omega) &= \bar{\alpha} \Delta_{h_x} \frac{4\lambda \Delta_B + \Delta_{\dot{\Psi}}}{\lambda\omega} \end{aligned}$$

Moreover, it is easy to show from Lemma B.6 that

$$\left\| \int_0^t e^{-2\lambda(t-\nu)} \Phi_3(x, x_r) d\nu \right\| \leq \frac{\Delta_\theta \rho_\gamma}{2\sqrt{\Gamma}},$$

for all $t \in [0, \tau^*]$, where

$$\Delta_\theta := \frac{\Delta_B \bar{\alpha} \Delta_{\tilde{\eta}}}{\lambda}. \quad (\text{A.10})$$

Therefore we obtain the following bound on the Riemannian energy

$$\mathcal{E}(x_r, x) \leq \zeta_2(\omega) \rho_\gamma^2 + \zeta_3(\omega) \rho_\gamma^2 + \frac{\Delta_\theta \rho_\gamma}{\sqrt{\Gamma}}.$$

Recall from the contradiction argument that $\|x_r(\tau^*) - x(\tau^*)\| = \rho_\gamma$. Since $\mathcal{E}(x_r, x) \geq \underline{\alpha} \|x_r(t) - x(t)\|^2$ from [17, Lemma 3.7], the following inequality must be satisfied

$$\underline{\alpha} \rho_\gamma^2 \leq \zeta_2(\omega) \rho_\gamma^2 + \zeta_3(\omega) \rho_\gamma^2 + \frac{\Delta_\theta \rho_\gamma}{\sqrt{\Gamma}} \implies \sqrt{\Gamma} \leq \frac{\Delta_\theta}{\rho_\gamma (\underline{\alpha} - \zeta_2(\omega) - \zeta_3(\omega))}.$$

However, from Eq. (18c) the adaptation rate is chosen such that

$$\sqrt{\Gamma} > \frac{\Delta_\theta}{\rho_\gamma (\underline{\alpha} - \zeta_2(\omega) - \zeta_3(\omega))}.$$

This directly contradicts our earlier statement, and therefore $\|x_r - x\|_{\mathcal{L}_\infty}^{[0, \tau]} < \rho_\gamma$ for any $\tau \geq 0$. \square

Proof of Theorem 5.1. We will prove this by contradiction: assume that

$$\|x^* - x\|_{\mathcal{L}_\infty} \geq \rho.$$

From the first filter bandwidth condition in Eq. (18a), we have $\|x^*(0) - x(0)\| < \rho$. Then there must exist a $\tau^* > 0$ such that

$$\begin{aligned} \|x^*(\tau^*) - x(\tau^*)\| &= \rho, \\ \|x^*(t) - x(t)\| &< \rho, \quad t \in [0, \tau^*). \end{aligned}$$

According to Lemma 5.1, we have $\|x^* - x_r\|_{\mathcal{L}_\infty} \leq \rho_r$, and from Lemma 5.2 it follows that $\|x_r - x\|_{\mathcal{L}_\infty}^{[0, \tau^*]} < \rho_\gamma$. Therefore, from triangle inequality we have $\|x^* - x\|_{\mathcal{L}_\infty}^{[0, \tau^*]} < \rho_r + \rho_\gamma \leq \rho$. This directly contradicts our assumption, and therefore $\|x^* - x\|_{\mathcal{L}_\infty} < \rho$. Additionally, from Lemma 5.1 the reference system satisfies a uniform ultimate bound given by $\|x^*(t) - x(t)\| \leq \epsilon(\omega, T)$ for all $t \geq T \geq 0$. Therefore, $\|x^*(t) - x(t)\| < \epsilon(\omega, T) + \rho_\gamma$ for all $t \geq T \geq 0$. \square

B Technical Results

Lemma B.1. Consider a scalar system with vector inputs

$$\begin{aligned} \dot{z}(t) &= -az(t) + b(t)^\top \xi(t), \quad z(0) = 0, \\ \xi(s) &= (1 - C(s))\sigma(s), \end{aligned}$$

where $z(t) \in \mathbb{R}$ is the state, $\sigma(t) \in \mathbb{R}^m$ is the control input with a column vector of transfer functions $\sigma(s)$, $a > 0$ is a scalar, $b(t) \in \mathbb{R}^m$ is differentiable, and $C(s)$ is a low-pass filter of the form $\frac{\omega}{s+\omega}$ with bandwidth $\omega > 0$. If the following bounds hold

$$\|b\|_{\mathcal{L}_\infty}^{[0, \tau]} \leq \Delta_b, \quad \|\dot{\sigma}\|_{\mathcal{L}_\infty}^{[0, \tau]} \leq \Delta_{\sigma_t},$$

then the following inequality holds

$$\|z\|_{\mathcal{L}_\infty}^{[0, \tau]} \leq \Delta_b \left(\frac{\|\sigma(0)\|}{|a - \omega|} + \frac{\Delta_{\sigma_t}}{a\omega} \right).$$

Proof. The scalar system can be equivalently written as

$$\dot{z}(t) = -az(t) + b(t)^\top \xi(t) \quad z(0) = 0 \quad (\text{B.11})$$

$$\dot{\xi}(t) = -\omega\xi(t) + \dot{\sigma}(t), \quad \xi(0) = \sigma(0). \quad (\text{B.12})$$

The solution to the differential equation in Eq. (B.12) is

$$\xi(\lambda) = e^{-\omega\lambda}\sigma(0) + \int_0^\lambda e^{-\omega(\lambda-\nu)}\dot{\sigma}(\nu) d\nu,$$

and the solution to Eq. (B.11) is

$$z(t) = \int_0^t e^{-a(t-\lambda)} b(\lambda)^\top \xi(\lambda) d\lambda.$$

Combining the equations above, we have

$$\|z(t)\| \leq \Delta_b \frac{\|\sigma(0)\|(e^{-\omega t} - e^{-at})}{a - \omega} + \Delta_b \frac{\Delta_{\sigma_t}}{\omega} \left(\frac{1 - e^{-at}}{a} - \frac{e^{-\omega t} - e^{-at}}{a - \omega} \right).$$

Ignoring the terms that are always less than zero, this is further bounded as

$$\|z(t)\| \leq \Delta_b \left(\frac{\|\sigma(0)\|}{|a - \omega|} + \frac{\Delta_{\sigma_t}}{a\omega} \right),$$

for all $t \in [0, \tau]$. \square

Lemma B.2. Consider a scalar system with vector inputs

$$\begin{aligned} \dot{z}(t) &= -az(t) + b(t)^\top \xi(t), \quad z(0) = 0, \\ \xi(s) &= (1 - C(s))\sigma(s), \end{aligned}$$

where $z(t) \in \mathbb{R}$ is the state, $\sigma(t) \in \mathbb{R}^m$ is the control input with a column vector of transfer functions $\sigma(s)$, $a > 0$ is a scalar, $b(t) \in \mathbb{R}^m$ is differentiable, and $C(s)$ is a low-pass filter of the form $\frac{\omega}{s+\omega}$ with bandwidth $\omega > 0$. If the following bounds hold

$$\|b\|_{\mathcal{L}_\infty}^{[0,\tau]} \leq \Delta_b, \quad \|\dot{b}\|_{\mathcal{L}_\infty}^{[0,\tau]} \leq \Delta_{b_t}, \quad \|\sigma\|_{\mathcal{L}_\infty}^{[0,\tau]} \leq \Delta_\sigma,$$

for all $t \in [0, \tau]$, then the following inequality holds

$$\|z\|_{\mathcal{L}_\infty}^{[0,\tau]} \leq \Delta_\sigma \frac{2a\Delta_b + \Delta_{b_t}}{a\omega},$$

for all $t \in [0, \tau]$.

Proof. We closely follow the analysis in [9, Lemma 1], but show that the inequality holds for vector inputs as well. Since the input is bounded in truncation, the norm of the system solution is bounded as

$$\|z\|_{\mathcal{L}_\infty}^{[0,\tau]} \leq \|\mathcal{Y}\|_{\mathcal{L}_1}^{[0,\tau]} \|\sigma\|_{\mathcal{L}_\infty}^{[0,\tau]},$$

where \mathcal{Y} is the equivalent of a transfer function between σ and z [19, Lemma A.7.1]. The impulse response $y(t)$ of \mathcal{Y} to the Dirac delta function $\delta(t)$ is characterized as

$$\begin{aligned} y(t) &= \int_0^t e^{-a(t-\lambda)} b(\lambda)^\top \int_0^\lambda \mathbb{1}_m(\delta(\nu) - \omega e^{-\omega\nu}) \delta(\lambda - \nu) d\nu d\lambda \\ &= \int_0^t e^{-a(t-\lambda)} b(\lambda)^\top \mathbb{1}_m(\delta(\lambda) - \omega e^{-\omega\lambda}) d\lambda \\ &= e^{-at} b(0)^\top \mathbb{1}_m - \int_0^t e^{-a(t-\lambda)} b(\lambda)^\top \mathbb{1}_m \omega e^{-\omega\lambda} d\lambda. \end{aligned}$$

Integrating the second term by parts we obtain the solution of the system as

$$y(t) = e^{-\omega t} b(t)^\top \mathbb{1}_m - \int_0^t \left(e^{-a(t-\lambda)} \dot{b}(\lambda) - a e^{-a(t-\lambda)} b(\lambda) \right)^\top \mathbb{1}_m e^{-\omega\lambda} d\lambda.$$

The \mathcal{L}_1 norm of \mathcal{Y} is simply the norm of the impulse response, which is given by

$$\begin{aligned} \mathcal{Y}_{\mathcal{L}_1}^{[0,\tau]} &= \|y\|_{\mathcal{L}_1}^{[0,\tau]} = \int_0^\tau \|y(t)\| dt \\ &= \int_0^\tau \left\| e^{-\omega t} b(t)^\top \mathbb{1}_m - \int_0^t \left(e^{-a(t-\lambda)} \dot{b}(\lambda) - a e^{-a(t-\lambda)} b(\lambda) \right)^\top \mathbb{1}_m e^{-\omega\lambda} d\lambda \right\| dt \\ &\leq \Delta_b \frac{1 - e^{-\omega\tau}}{\omega} + \int_0^\tau \left\| \int_0^t \left(e^{-a(t-\lambda)} \dot{b}(\lambda) - a e^{-a(t-\lambda)} b(\lambda) \right)^\top \mathbb{1}_m e^{-\omega\lambda} d\lambda \right\| dt \\ &\leq \Delta_b \frac{1 - e^{-\omega\tau}}{\omega} + (\Delta_{b_t} + a\Delta_b) \int_0^\tau \int_0^t e^{-a(t-\lambda)} e^{-\omega\lambda} d\lambda dt \\ &\leq \Delta_b \frac{1 - e^{-\omega\tau}}{\omega} + (\Delta_{b_t} + a\Delta_b) \left(\frac{1}{a\omega} - \frac{ae^{-\omega\tau} - \omega e^{-a\tau}}{a\omega(a - \omega)} \right). \end{aligned}$$

Ignoring terms which are always less than zero, this norm can be further upper bounded

$$\mathcal{Y}_{\mathcal{L}_1}^{[0,\tau]} \leq \frac{2a\Delta_b + \Delta_{b_t}}{a\omega}$$

Therefore, the solution of the system $z(t)$ is bounded as

$$z(t) \leq \Delta_\sigma \frac{2a\Delta_b + \Delta_{b_t}}{a\omega},$$

for all $t \in [0, \tau]$. □

Lemma B.3. Consider two states $x_0, x_1 \in \mathcal{X}$ and a minimizing geodesic $\bar{\gamma} : [0, 1] \rightarrow \mathcal{X}$ under the metric $M(x)$ such that $\bar{\gamma}(0) = x_0$ and $\bar{\gamma}(1) = x_1$. Then the following inequalities are satisfied

$$\|M(\bar{\gamma}(s))\bar{\gamma}_s(s)\| \leq \bar{\alpha} \|x_0 - x_1\|, \quad (\text{B.13})$$

$$\|\bar{\gamma}_s(s)\| \leq \sqrt{\frac{\bar{\alpha}}{\underline{\alpha}}} \|x_0 - x_1\|, \quad (\text{B.14})$$

for all $s \in [0, 1]$, where $\Theta(x)^\top \Theta(x) = M(x)$. Further, there exists $\bar{\alpha} \geq \underline{\alpha} > 0$ such that $\bar{\alpha} \mathbb{I}_n \succeq M(x) \succeq \underline{\alpha} \mathbb{I}_n$.

Proof. In [14, Theorem 1], the authors show that the length of the minimizing geodesic $d(x_0, x_1)$ is bounded as

$$\sqrt{\underline{\alpha}}\|x_0 - x_1\| \leq d(x_0, x_1) \leq \sqrt{\bar{\alpha}}\|x_0 - x_1\|,$$

if the metric $M(x)$ is uniformly bounded as given in the lemma's statement. Geodesics exhibit the special property [34, Lemma 5.5] that $\bar{\gamma}_s(s)^\top M(\bar{\gamma}_s(s))\bar{\gamma}_s(s) = c > 0$ for all $s \in [0, 1]$, i.e. they are of constant speed. Since $s \in [0, 1]$, the speed of a geodesic is also the length of the geodesic

$$\sqrt{\bar{\gamma}_s(s)^\top M(\bar{\gamma}_s(s))\bar{\gamma}_s(s)} = d(x_0, x_1) \leq \sqrt{\bar{\alpha}}\|x_0 - x_1\|, \quad (\text{B.15})$$

for all $s \in [0, 1]$. Therefore given the factorization $M(x) = \Theta(x)^\top \Theta(x)$ we obtain the following inequality

$$\|\Theta(\bar{\gamma}(s))\bar{\gamma}_s(s)\| \leq \sqrt{\bar{\alpha}}\|x_0 - x_1\|.$$

Since $\|M(\bar{\gamma}(s))\bar{\gamma}_s(s)\| \leq \|\Theta(\bar{\gamma}(s))^\top\| \|\Theta(\bar{\gamma}(s))\bar{\gamma}_s(s)\|$ (because of the submultiplicative property of induced matrix norms and $\|\Theta(x)\| \leq \sqrt{\bar{\alpha}}$ for all x), we arrive at Eq. (B.13). Additionally, since $M(x)$ is uniformly bounded, the following inequality holds

$$\underline{\alpha}\bar{\gamma}_s(s)^\top \mathbb{I}_n \bar{\gamma}_s(s) \leq \bar{\gamma}_s(s)^\top M(\bar{\gamma}(s))\bar{\gamma}_s(s),$$

for all $s \in [0, 1]$. Combining the above inequality with Eq. (B.15), we obtain the result in Eq. (B.14). \square

Lemma B.4. Consider two smooth trajectories x_0 and x_1 such that $x_0(t) \in \Omega(\rho, x^*(t))$ and $x_1(t) \in \Omega(\rho, x^*(t))$ for all $t \in [0, \tau]$, and a minimizing geodesic $\bar{\gamma}(\cdot, t) : [0, 1] \rightarrow \mathcal{X}$ under the metric $M(x)$ such that $\bar{\gamma}(0, t) = x_0(t)$ and $\bar{\gamma}(1, t) = x_1(t)$. Then we have

$$\|\bar{\gamma}_s(1, t)^\top M(\bar{\gamma}(1, t)) - \bar{\gamma}_s(0, t)^\top M(\bar{\gamma}(0, t))\| \leq \frac{\bar{\alpha}}{2\underline{\alpha}} \Delta_{M_x} \|x_0 - x_1\|^2,$$

for all $t \in [0, \tau]$.

Proof. From the fundamental theorem of calculus we know that

$$[M(\bar{\gamma}(s, t))\bar{\gamma}_s(s, t)]_{s=0}^{s=1} = \int_0^1 \frac{\partial}{\partial s} (\bar{\gamma}_s(s, t)^\top M(\bar{\gamma}(s, t))) \, ds.$$

Recall that the differential Lyapunov function is defined as $V(x, \delta x) := \delta x^\top M(x) \delta x$. Then the equation above satisfies

$$[M(\bar{\gamma}(s, t))\bar{\gamma}_s(s, t)]_{s=0}^{s=1} = \frac{1}{2} \int_0^1 \frac{\partial}{\partial s} \frac{\partial V}{\partial \delta x} (\bar{\gamma}(s, t), \bar{\gamma}_s(s, t)) \, ds$$

Since $\bar{\gamma}$ is the minimizing geodesic, it must satisfy the Euler-Lagrange equation given by

$$[M(\bar{\gamma}(s, t))\bar{\gamma}_s(s, t)]_{s=0}^{s=1} = \frac{1}{2} \int_0^1 \frac{\partial V}{\partial x} (\bar{\gamma}(s, t), \bar{\gamma}_s(s, t)) \, ds.$$

It follows from the definition of the differential Lyapunov function, the following is satisfied component-wise

$$[M(\bar{\gamma}(s, t))\bar{\gamma}_s(s, t)]_{s=0}^{s=1}[i] = \frac{1}{2} \int_0^1 \bar{\gamma}_s(s, t)^\top \frac{\partial M}{\partial x_i} (\bar{\gamma}(s, t)) \bar{\gamma}_s(s, t) \, ds.$$

From Eq. (A.8) and Lemma B.3 the following bounds hold

$$\sum_{i=1}^n \left\| \frac{\partial M}{\partial x_i}(x) \right\| \leq \Delta_{M_x}, \quad \|\bar{\gamma}_s(s, t)\|^2 \leq \frac{\bar{\alpha}}{\underline{\alpha}} \|x_0 - x_1\|^2$$

for all $x(t) \in \Omega(\rho, x^*(t))$ and $t \in [0, \tau]$, and we arrive at the result. \square

Lemma B.5. If the state trajectory of the reference system in Eq. (19) satisfies $x_r(t) \in \Omega(\rho, x^*(t))$ for all $t \in [0, \tau]$ and the state trajectory of the real system in Eq. (1) with control input Eq. (10) satisfies $x(t) \in \Omega(\rho, x^*(t))$ for all $t \in [0, \tau]$, then the following inequalities are satisfied

$$\|\dot{x}_r\|_{\mathcal{L}_\infty}^{[0, \tau]} \leq \Delta_{\dot{x}_r} := \Delta_f + \Delta_B(\Delta_h + \Delta_{u^*} + \rho\Delta_{\delta_u}), \quad (\text{B.16})$$

$$\|\dot{x}\|_{\mathcal{L}_\infty}^{[0, \tau]} \leq \Delta_{\dot{x}} := \Delta_f + \Delta_B(2\Delta_h + \Delta_{u^*} + \rho\Delta_{\delta_u}), \quad (\text{B.17})$$

where the CCM control effort is uniformly bounded by Δ_{δ_u} defined by the following inequality

$$\Delta_{\delta_u} \geq \frac{1}{2} \sup_{x \in \Omega(\rho, x^*(t))} \left(\frac{\bar{\lambda}(L^{-\top}(x)F(x)L^{-1}(x))}{\underline{\sigma}_{>0}(B^\top(x)L^{-1}(x))} \right), \quad (\text{B.18})$$

for all $t \geq 0$, and $L(x)$ is obtained from the factorization of the dual metric $W(x)$, i.e., $L(x)^\top L(x) = W(x)$, and the matrix $F(x)$ is defined as

$$F(x) := -\partial_f W(x) + 2 \left[\frac{\partial f}{\partial x}(x) W(x) \right]_{\mathbb{S}} + 2\lambda W(x).$$

Proof. Since induced matrix norms are subordinate to Euclidean vector norms, we have

$$\|\dot{x}_r(t)\| \leq \Delta_f + \Delta_B \left(\|\tilde{h}(t, x_r)\| + \|u_c(t, x)\| \right),$$

for all $t \in [0, \tau]$, where $\tilde{h}(t, x_r) = h(t, x_r) - \eta_r(t)$. Moreover, $\mathcal{L}[\tilde{h}(t, x_r)] = \mathcal{L}[h(t, x_r) - \eta_r(t)] = (1 - C(s))\mathcal{L}[h(t, x_r)]$. From [19, Lemma A.7.1] we know that $\|\tilde{h}(t, x_r)\| \leq \|1 - C(s)\|_{\mathcal{L}_1} \Delta_h$. Moreover, it can be verified for first order filters of the form $C(s) = \frac{\omega}{s + \omega}$ that $\|C(s)\|_{\mathcal{L}_1} = \|1 - C(s)\|_{\mathcal{L}_1} = 1$, which implies that $\|\tilde{h}(t, x_r)\| \leq \Delta_h$ for all $t \in [0, \tau]$. From Assumption 2.2, $\|u^*(t)\| \leq \Delta_{u^*}$ for all $t \in [0, \tau]$, and from [17, Theorem 5.2], the control effort exerted by CCM-based controller is bounded by Eq. (B.18). We arrive thus at the result in Eq. (B.16). Similar to the reasoning above, the real system dynamics satisfies

$$\|\dot{x}_r(t)\| \leq \Delta_f + \Delta_B (\|h(t, x)\| + \|u_a(t)\| + \|u_c(t, x)\|),$$

for all $t \in [0, \tau]$. Additionally, $\|u_a(t)\| \leq \|C(s)\|_{\mathcal{L}_1} \Delta_h$ because the projection operator in the adaptation law will ensure that $\|\hat{\sigma}(t)\| \leq \Delta_h$ for all $t > 0$. However, since $\|C(s)\|_{\mathcal{L}_1} = 1$, $\|h(t, x)\| \leq \Delta_h$, and $\|u_c(t, x)\| \leq \Delta_{u^*} + \rho \Delta_{\delta_u}$ we obtain Eq. (B.17). \square

Lemma B.6. *If the state trajectory of the real system in Eq. (1) with control input Eq. (10) satisfies $x(t) \in \Omega(\rho, x^*(t))$ for all $t \in [0, \tau]$, then the error in the state predictor satisfies the following inequalities*

$$\|\tilde{x}\|_{\mathcal{L}_\infty}^{[0, \tau]} \leq \frac{\Delta_{\tilde{x}}}{\sqrt{\Gamma}}, \quad (\text{B.19})$$

$$\|\tilde{\eta}\|_{\mathcal{L}_\infty}^{[0, \tau]} \leq \frac{\Delta_{\tilde{\eta}}}{\sqrt{\Gamma}}, \quad (\text{B.20})$$

where

$$\begin{aligned} \Delta_{\tilde{x}} &:= \sqrt{\frac{4\bar{\lambda}(P)\Delta_h(\Delta_{h_t} + \Delta_{h_x}\Delta_{\tilde{x}})}{\underline{\lambda}(P)\underline{\lambda}(Q)} + \frac{4\Delta_h^2}{\underline{\lambda}(P)}}, \\ \Delta_{\tilde{\eta}} &:= \left(\Delta_{B_x^\top} \Delta_{\tilde{x}} + (\omega + \|A_m\|) \Delta_{B^\top} \right) \Delta_{\tilde{x}}. \end{aligned}$$

Proof. The state predictor error dynamics is given by

$$\dot{\tilde{x}}(t) = A_m \tilde{x}(t) + B(x) \tilde{\sigma}(t), \quad \tilde{x}(0) = 0,$$

where $\tilde{\sigma}(t) = \hat{\sigma}(t) - h(t, x)$. Consider the Lyapunov function $V(\tilde{x}, \tilde{\sigma}) = \tilde{x}(t)^\top P \tilde{x}(t) + \tilde{\sigma}(t)^\top \Gamma^{-1} \tilde{\sigma}(t)$. Then its time derivative is given by

$$\dot{V}(\tilde{x}, \tilde{\sigma}) = -\tilde{x}(t)^\top Q \tilde{x}(t) + 2\tilde{\sigma}(t)^\top B(x)^\top P \tilde{x}(t) + 2\tilde{\sigma}(t)^\top \Gamma^{-1} (\dot{\hat{\sigma}}(t) - \dot{h}(t, x)),$$

where $P \succ 0$ and $Q \succ 0$ define the adaptation law in Eq. (14). Combing the adaptation law with the equation above, we obtain

$$\dot{V}(\tilde{x}, \tilde{\sigma}) = -\tilde{x}(t)^\top Q \tilde{x}(t) + 2\tilde{\sigma}(t)^\top (B(x)^\top P \tilde{x}(t) + \text{Proj}_{\mathcal{H}}(\hat{\sigma}(t), -B(x)^\top P \tilde{x}(t)) - 2\tilde{\sigma}(t)^\top \Gamma^{-1} \dot{h}(t, x)).$$

The projection operator satisfies an important property [28, Lemma 6], which ensures that since $h(t, x) \in \mathcal{H}$ always, we have $\tilde{\sigma}(t)^\top (\text{Proj}_{\mathcal{H}}(\hat{\sigma}(t), y(t)) - y(t)) \leq 0$, where $y(t) = -B(x)^\top P \tilde{x}(t)$. Therefore, the equation above reduces to

$$\dot{V}(\tilde{x}, \tilde{\sigma}) \leq -\tilde{x}(t)^\top Q \tilde{x}(t) - 2\tilde{\sigma}(t)^\top \Gamma^{-1} \dot{h}(t, x).$$

It is easy to show that $\|\tilde{\sigma}(t)\| \leq 2\Delta_h$ for all $t \geq 0$ we have $-\tilde{x}(t)Q\tilde{x}(t) \leq -\lambda(Q)\|\tilde{x}(t)\|^2$, and from Lemma B.5 we know that $\|\dot{h}(t, x)\| \leq \Delta_{h_t} + \Delta_{h_x}\Delta_{\dot{x}}$ for all $t \in [0, \tau]$. Combining, these bounds with the equation above results in the following inequality

$$\dot{V}(\tilde{x}, \tilde{\sigma}) \leq -\lambda(Q)\|\tilde{x}\|^2 + 4\Delta_h\Gamma^{-1}(\Delta_{h_t} + \Delta_{h_x}\Delta_{\dot{x}}).$$

Now, if $\dot{V}(\tilde{x}(t), \tilde{\sigma}(t)) \geq 0$, then

$$\|\tilde{x}(t)\|^2 \leq \frac{4\Delta_h(\Delta_{h_t} + \Delta_{h_x}\Delta_{\dot{x}})}{\Gamma\lambda(Q)}, \quad (\text{B.21})$$

for all $t \in [0, \tau]$. Otherwise $\dot{V}(\tilde{x}(t), \tilde{\sigma}(t)) < 0$. However, the Lyapunov function always remains bounded as

$$\lambda(P)\|\tilde{x}(t)\|^2 \leq V(\tilde{x}(t), \tilde{\sigma}(t)) \leq \bar{\lambda}(P)\|\tilde{x}(t)\|^2 + 4\Delta_h^2\Gamma^{-1}.$$

Combining the equation above with Eq. (B.21), we arrive at the result in Eq. (B.20). In order to show that the inequality in Eq. (B.20) holds, we start with the error in the uncertainty estimate from the state predictor error dynamics in terms of the Moore-Penrose inverse of $B(x)$ as

$$\tilde{\sigma}(t) = B^\dagger(x)\dot{\tilde{x}}(t) - B^\dagger(x)A_m\tilde{x}(t).$$

Since $\tilde{\eta}(s) = C(s)\tilde{\sigma}(s)$, we obtain

$$\begin{aligned} \tilde{\eta}(s) &= C(s)\mathcal{L}[B^\dagger(x)\dot{\tilde{x}}(t) - B^\dagger(x)A_m\tilde{x}(t)] \\ &= C(s)\mathcal{L}\left[\frac{dB^\dagger(x)\tilde{x}(t)}{dt} - \frac{dB^\dagger(x)}{dt}\tilde{x}(t) - B^\dagger(x)A_m\tilde{x}(t)\right] \\ &= C(s)s\mathcal{L}[B^\dagger(x)\tilde{x}(t)] + C(s)\mathcal{L}\left[-\frac{dB^\dagger(x)}{dt}\tilde{x}(t) - B^\dagger(x)A_m\tilde{x}(t)\right]. \end{aligned}$$

From Lemma B.5 we know $\left\|\frac{dB^\dagger(x)}{dt}\right\| = \left\|\sum_{j=0}^n \frac{\partial B^\dagger(x)}{\partial x_j} \dot{x}_j(t)\right\| \leq \Delta_{B_x^\dagger}\Delta_{\dot{x}}$ and $\|B^\dagger(x)\| \leq \Delta_{B^\dagger}$ for all $x \in \Omega(\rho, x^*(t))$ and $t \in [0, \tau]$. Therefore, using the property from [19, Lemma A.7.1], the following inequality holds

$$\|\tilde{\eta}(t)\| \leq \left(\|C(s)s\|_{\mathcal{L}_1}\Delta_{B^\dagger} + \|C(s)\|_{\mathcal{L}_1}\left(\Delta_{B_x^\dagger}\Delta_{\dot{x}} + \Delta_{B^\dagger}\|A_m\|\right)\right)\frac{\Delta_{\tilde{x}}}{\sqrt{1}},$$

for all $x \in \Omega(\rho, x^*(t))$ and $t \in [0, \tau]$. Since $\|C(s)s\|_{\mathcal{L}_1} = \omega$ and $\|C(s)\|_{\mathcal{L}_1} = 1$, we prove the result. \square

Lemma B.7. *If the state trajectory of the real system in Eq. (1) with control (10) satisfies $x(t) \in \Omega(\rho, x^*(t))$ and the reference system in Eq. (19) satisfies $x_r(t) \in \Omega(\rho, x^*(t))$ for $t \in [0, \tau]$, then the following inequality holds*

$$\left\|\frac{d}{dt}(B(x)^\top M(x)\bar{\gamma}_s(0, t))\right\| \leq \Delta_{\dot{\Psi}}\|x_r(t) - x(t)\|,$$

where

$$\begin{aligned} \Delta_{\dot{\Psi}} &:= \bar{\alpha} \left(\Delta_B \Delta_{\bar{\gamma}_{s_t}} + \frac{\Delta_B \Delta_{M_x} \Delta_{\dot{x}}}{\sqrt{\bar{\alpha}\underline{\alpha}}} + \Delta_{B_x} \Delta_{\dot{x}} \right), \\ \Delta_{\bar{\gamma}_{s_t}} &:= \sqrt{\frac{\bar{\alpha}}{\underline{\alpha}}} \left(\Delta_{f_x} + (\Delta_h + \Delta_{u^*} + \rho \Delta_{\delta_u}) \Delta_{B_x} + \left(\Delta_{h_x} + \frac{\sqrt{\bar{\alpha}} \Delta_{\delta_u}}{\sqrt{\bar{\alpha}}} \right) \Delta_B \right), \end{aligned}$$

for all $t \in [0, \tau]$, where $\bar{\gamma}(\cdot, t) : [0, 1] \rightarrow \mathcal{X}$ is the minimizing geodesic under the metric $M(x)$ such that $\bar{\gamma}(0, t) = x(t)$ and $\bar{\gamma}(1, t) = x_r(t)$.

Proof. The time-derivative of the minimizing geodesic $\dot{\bar{\gamma}}_s(s, t)|_{s=0}$ is given by the variational dynamics at $x(t)$ as follows

$$\dot{\bar{\gamma}}_s(0, t) = \left(\left[\frac{\partial f(x)}{\partial x} + \sum_{j=1}^m (u_j(t) + h_j(t, x)) \frac{\partial b_j(x)}{\partial x} \right] + B(x) \frac{\partial h(t, x)}{\partial x} \right) \bar{\gamma}_s(0, t) + B(x) \delta_u, \quad (\text{B.22})$$

where $b_j(x)$ is the j^{th} column of $B(x)$, $u_j(t)$ is the j^{th} value in control channel, and $h_j(t, x)$ is the j^{th} value of the uncertainty. Previously, from Assumptions 2.3 and 2.4 and Lemmas B.3 and B.5 we derived bounds for the following

terms

$$\begin{aligned} \left\| \frac{\partial f(x)}{\partial x} \right\| &\leq \Delta_{f_x}, \quad \|B(x)\| \leq \Delta_B, \quad \sum_{j=1}^m \left\| \frac{\partial b_j(x)}{\partial x} \right\| \leq \Delta_{B_x}, \\ \|h(t, x)\| &\leq \Delta_h, \quad \left\| \frac{\partial h(t, x)}{\partial x} \right\| \leq \Delta_{h_x}, \\ \|u(t)\| &\leq \Delta_{u^*} + \Delta_h + \rho \Delta_{\delta_u}, \quad \|\bar{\gamma}_s(1, t)\| \leq \sqrt{\frac{\bar{\alpha}}{\underline{\alpha}}} \|x_r(t) - x(t)\|, \end{aligned}$$

for all $x \in \Omega(\rho, x^*(t))$ and $t \geq 0$. Additionally, from Lemma B.5 the differential state feedback from Eq. (B.18) is bounded by $\|\delta_u\| \leq \Delta_{\delta_u} \|x(t) - x_r(t)\|$. With these considerations, the expression in Eq. (B.22) is uniformly bounded as

$$\begin{aligned} \|\dot{\bar{\gamma}}_s(0, t)\| &\leq \sqrt{\frac{\bar{\alpha}}{\underline{\alpha}}} \left(\Delta_{f_x} + (\Delta_h + \Delta_{u^*} + \rho \Delta_{\delta_u}) \Delta_{B_x} + \left(\Delta_{h_x} + \frac{\sqrt{\bar{\alpha}} \Delta_{\delta_u}}{\sqrt{\underline{\alpha}}} \right) \Delta_B \right) \|x_r(t) - x(t)\| \\ &= \Delta_{\bar{\gamma}_{s_t}} \|x_r(t) - x(t)\|, \end{aligned}$$

for all $t \in [0, \tau]$. Next we compute the bounds on $\left\| \frac{d}{dt} (B(x)^\top M(x) \bar{\gamma}_s(0, t)) \right\|$ using Lemmas B.3, B.5 and B.7 and Assumptions 2.3 and 2.4 as follows

$$\begin{aligned} \left\| \frac{d}{dt} (B(x)^\top M(x) \bar{\gamma}_s(0, t)) \right\| &\leq \|B(x)^\top M(x) \dot{\bar{\gamma}}_s(0, t) + B(x)^\top \partial_{\dot{x}(t)} M(x) \bar{\gamma}_s(0, t) + \partial_{\dot{x}(t)} B(x)^\top M(x) \bar{\gamma}_s(0, t)\|, \\ &\leq \bar{\alpha} \left(\Delta_B \Delta_{\bar{\gamma}_{s_t}} + \frac{\Delta_B \Delta_{M_x} \Delta_{\dot{x}}}{\sqrt{\bar{\alpha} \underline{\alpha}}} + \Delta_{B_x} \Delta_{\dot{x}} \right) \|x_r(t) - x(t)\|, \end{aligned}$$

and we arrive at the result of the lemma. \square

References

- [1] S. M. LaValle, *Planning algorithms*. Cambridge University Press, 2006.
- [2] R. E. Mahony, V. Kumar, and P. I. Corke, “Multirotor aerial vehicles: Modeling, estimation, and control of quadrotor,” *IEEE Robotics & Automation Magazine*, vol. 19, pp. 20–32, 2012.
- [3] R. Mahony and T. Hamel, “Robust trajectory tracking for a scale model autonomous helicopter,” *International Journal of Robust and Nonlinear Control: IFAC-Affiliated Journal*, vol. 14, no. 12, pp. 1035–1059, 2004.
- [4] S. Jeong and D. Chwa, “Coupled multiple sliding-mode control for robust trajectory tracking of hovercraft with external disturbances,” *IEEE Transactions on Industrial Electronics*, vol. 65, no. 5, pp. 4103–4113, 2017.
- [5] A. Donaire, J. G. Romero, and T. Perez, “Trajectory tracking passivity-based control for marine vehicles subject to disturbances,” *Journal of the Franklin Institute*, vol. 354, no. 5, pp. 2167–2182, 2017.
- [6] H. K. Khalil and J. W. Grizzle, *Nonlinear systems*. Prentice Hall Upper Saddle River, NJ, 2002, vol. 3.
- [7] L. Magni, H. Nijmeijer, and A. van der Schaft, “A receding-horizon approach to the nonlinear H_∞ control problem,” *Automatica*, vol. 37, pp. 429–435, 2001.
- [8] D. M. Raimondo, D. Limon, M. Lazar, L. Magni, and E. F. Camacho, “Min-max model predictive control of nonlinear systems: A unifying overview on stability,” *European Journal of Control*, vol. 15, no. 1, pp. 5–21, 2009.
- [9] X. Wang, L. Yang, Y. Sun, and K. Deng, “Adaptive model predictive control of nonlinear systems with state-dependent uncertainties,” *International Journal of Robust and Nonlinear Control*, vol. 27, no. 17, pp. 4138–4153, 2017.
- [10] S. V. Raković, “Set theoretic methods in model predictive control,” in *Nonlinear Model Predictive Control*. Springer, 2009, pp. 41–54.
- [11] S. V. Raković, W. S. Levine, and B. Açıkmeşe, “Elastic tube model predictive control,” in *2016 American Control Conference (ACC)*. IEEE, 2016, pp. 3594–3599.
- [12] S. Yu, C. Böhm, H. Chen, and F. Allgöwer, “Robust model predictive control with disturbance invariant sets,” in *Proceedings of the 2010 American Control Conference*. IEEE, 2010, pp. 6262–6267.
- [13] B. T. Lopez, J. P. How, and J.-J. E. Slotine, “Dynamic tube MPC for nonlinear systems,” in *Proceedings of the 2019 American Control Conference*. IEEE, 2019, pp. 1655–1662.

- [14] I. R. Manchester and J.-J. E. Slotine, “Control contraction metrics: Convex and intrinsic criteria for nonlinear feedback design,” *IEEE Transactions on Automatic Control*, vol. 62, no. 6, pp. 3046–3053, 2017.
- [15] I. R. Manchester, J. Z. Tang, and J.-J. E. Slotine, “Unifying robot trajectory tracking with control contraction metrics,” in *Robotics Research*. Springer, 2018, pp. 403–418.
- [16] W. Lohmiller and J.-J. E. Slotine, “On contraction analysis for non-linear systems,” *Automatica*, vol. 34, no. 6, pp. 683–696, 1998.
- [17] S. Singh, B. Landry, A. Majumdar, J.-J. Slotine, and M. Pavone, “Robust feedback motion planning via contraction theory,” *The International Journal of Robotics Research*, 2019, submitted.
- [18] B. T. Lopez and J.-J. E. Slotine, “Contraction metrics in adaptive nonlinear control,” *arXiv preprint arXiv:1912.13138*, 2019.
- [19] N. Hovakimyan and C. Cao, *\mathcal{L}_1 Adaptive Control Theory: Guaranteed Robustness with Fast Adaptation*. SIAM, 2010.
- [20] I. Gregory, E. Xargay, C. Cao, and N. Hovakimyan, “Flight test of an \mathcal{L}_1 adaptive controller on the NASA AirSTAR flight test vehicle,” in *Proceedings of AIAA Guidance, Navigation, and Control Conference*, Toronto, Ontario, Canada, August 2010, AIAA 2010-8015.
- [21] K. A. Ackerman, E. Xargay, R. Choe, N. Hovakimyan, M. C. Cotting, R. B. Jeffrey, M. P. Blackstun, T. P. Fulkerson, T. R. Lau, and S. S. Stephens, “Evaluation of an \mathcal{L}_1 adaptive flight control law on Calspan’s variable-stability Learjet,” *AIAA Journal of Guidance, Control, and Dynamics*, vol. 40, no. 4, pp. 1051–1060, 2017.
- [22] I. Kaminer, A. Pascoal, E. Xargay, N. Hovakimyan, C. Cao, and V. Dobrokhodov, “Path following for small unmanned aerial vehicles using \mathcal{L}_1 adaptive augmentation of commercial autopilots,” *AIAA Journal of Guidance, Control, and Dynamics*, vol. 33, no. 2, pp. 550–564, 2010.
- [23] H. Jafarnejadsani, D. Sun, H. Lee, and N. Hovakimyan, “Optimized \mathcal{L}_1 adaptive controller for trajectory tracking of an indoor quadrotor,” *AIAA Journal of Guidance, Control, and Dynamics*, vol. 40, no. 6, pp. 1415–1427, 2017.
- [24] X. Wang and N. Hovakimyan, “ \mathcal{L}_1 adaptive controller for nonlinear time-varying reference systems,” *Systems & Control Letters*, vol. 61, no. 4, pp. 455–463, 2012.
- [25] F. Bullo and A. D. Lewis, *Geometric Control of Mechanical Systems: Modeling, Analysis, and Design for Simple Mechanical Control Systems*. Springer, 2019, vol. 49.
- [26] P. E. Crouch and A. J. van der Schaft, *Variational and Hamiltonian control systems*. Springer, 1987.
- [27] M. P. Do Carmo, *Riemannian geometry*. Birkhäuser, 1992.
- [28] E. Lavretsky, T. E. Gibson, and A. M. Annaswamy, “Projection operator in adaptive systems,” *arXiv preprint arXiv:1112.4232*, 2011.
- [29] J.-B. Pomet and L. Praly, “Adaptive nonlinear regulation: Estimation from the Lyapunov equation,” *IEEE Transactions on Automatic Control*, vol. 37, no. 6, pp. 729–740, 1992.
- [30] C. Cao and N. Hovakimyan, “Stability margins of \mathcal{L}_1 adaptive control architecture,” *IEEE Transactions on Automatic Control*, vol. 55, no. 2, pp. 480–487, 2010.
- [31] S. Singh, A. Majumdar, J.-J. Slotine, and M. Pavone, “Robust online motion planning via contraction theory and convex optimization,” in *2017 IEEE International Conference on Robotics and Automation (ICRA)*, 2017, pp. 5883–5890.
- [32] K. Leung and I. R. Manchester, “Nonlinear stabilization via control contraction metrics: A pseudospectral approach for computing geodesics,” in *2017 American Control Conference (ACC)*. IEEE, 2017, pp. 1284–1289.
- [33] J. Bouvrie and J.-J. Slotine, “Wasserstein contraction for stochastic nonlinear systems,” *arXiv preprint arXiv:1902.08567*, 2019.
- [34] J. M. Lee, *Riemannian Manifolds: An Introduction to Curvature*. Springer Science & Business Media, 2006, vol. 176.